

Generalized Chaplygin Gas Models tested with SNIa

MAREK BIESIADA

Department of Astrophysics and Cosmology,

University of Silesia

Uniwersytecka 4, 40-007 Katowice, Poland

mb@imp.sosnowiec.pl

WŁODZIMIERZ GODŁOWSKI

Astronomical Observatory

Jagiellonian University

Orla171, Krakow, Poland

godlows@oa.uj.edu.pl

MAREK SZYDŁOWSKI

Astronomical Observatory

Jagiellonian University

Orla171, Krakow, Poland

szydlo@oa.uj.edu.pl

ABSTRACT

The so called Generalized Chaplygin Gas (GCG) with the equation of state $p = -\frac{A}{\rho^\alpha}$ was recently proposed as a candidate for dark energy in the Universe. In this paper we confront the GCG with SNIa data from Perlmutter et al. supplemented by more recent Knop sample.

Specifically we have tested the GCG cosmology in three different classes of models with (1) $\Omega_m = 0.3$, $\Omega_{Ch} = 0.7$; (2) $\Omega_m = 0.05$, $\Omega_{Ch} = 0.95$ and (3) $\Omega_m = 0$, $\Omega_{Ch} = 1$, as well a model without any assumption on Ω_m .

The best fitted models are obtained by minimalizing the χ^2 function which is illustrated by figures of residuals (with respect to Einstein-de Sitter model) and χ^2 levels in the (A_0, α) plane. We supplemented our analysis with confidence intervals in the (A_0, α) plane by marginalizing the probability density functions over remaining parameters assuming uniform priors. We have also derived one-dimensional probability distribution functions for Ω_{Ch} obtained from joint marginalization over α and A_0 . The maximum value of such PDF informs us about the most probable value of Ω_{Ch} (supported by supernovae data) within the full class of GCG models.

The general conclusion is that SNIa data strongly support the Chaplygin gas (with $\alpha = 1$). Moreover noticeable preference of A_0 values close to 1 means that

the α dependence becomes insignificant. It is reflected on one dimensional PDFs for α which turned out to be flat meaning that the power of present supernovae data to discriminate between various generalized Chaplygin gas models is weak. For comparison we repeated our analysis with Tonry/Barris sample of SNIa confirming the results obtained on Knop’s sample.

Extending our analysis by relaxing the flat prior lead to the result that even though the best fitted values of Ω_k are formally non-zero, still they are close to flat case. It should be viewed as an advantage of the GCG model since in similar analysis of Λ CDM model in (1) high negative value of Ω_k were found to be best fitted to the data and independent inspiration from CMBR and extragalactic astronomy has been invoked to fix the curvature problem.

Our results show clearly that in Generalized Chaplygin Gas cosmology distant $z > 1$ supernovae should be brighter than in Λ CDM model.

Therefore one can expect that future supernova experiments (e.g. SNAP) having access to higher redshifts will eventually resolve the issue whether the dark energy content of the Universe could be described as a Chaplygin gas. Moreover, we argue that with the future SNAP data it would be possible to differentiate between models with various value of α parameter and/or discriminated between GCG Cardassian and Λ CDM models. This discriminative power of forthcoming SNAP mission has been demonstrated on simulated SNAP data.

1. Introduction

For a couple of years two independent observational programs — the high redshift supernovae surveys (1) and CMBR small scale anisotropy measurements (2; 3) have brought a new picture of the Universe in the large. While interpreted within the FRW models results of these programs suggest that our Universe is flat (as inferred from the location of acoustic peaks in CMBR power spectrum) and presently accelerates its expansion (as inferred from the SNIa Hubble diagram). Combined with the independent knowledge about the amount of baryons and CDM estimated to be $\Omega_m = 0.3$ (4) it follows that about $\Omega_X = 0.7$ fraction of critical density $\rho_{cr} = \frac{3c^2 H_0^2}{8\pi G}$ should be contained in a mysterious component called “dark energy”. The most obvious candidate for this smooth component permeating the Universe is the cosmological constant Λ representing the energy of the vacuum. Well known fine tuning problems led many people to seek beyond the Λ framework, and the concept of the quintessence had been conceived. Usually the quintessence is described in a phenomenological manner, as a scalar field with an appropriate potential (5). It turns out, however, that quintessence program also suffers from its own fine tuning problems (6).

Recently the so called Chaplygin gas (7) — a hypothetical component with the equation of state $p = -\frac{A}{\rho}$ was proposed as a challenge to the above mentioned candidates for dark energy. This, also purely phenomenological, entity has interesting connections with string theory (8). Currently its generalizations admitting the equation of state $p = -\frac{A}{\rho^\alpha}$ where $0 \leq \alpha \leq 1$ have been proposed (9). In this paper we confront the Generalized Chaplygin Gas with the SNIa data.

2. Cosmological model

Einstein equations for the Friedman-Robertson-Walker model with hydrodynamical energy-momentum tensor $T_{\mu\nu} = (\rho + p)u_\mu u_\nu - pg_{\mu\nu}$ read:

$$\left(\frac{\dot{a}}{a}\right)^2 = \frac{8\pi G\rho}{3} - \frac{k}{a^2(t)} \quad (1)$$

$$\frac{\ddot{a}(t)}{a} = -\frac{4\pi G}{3}(\rho + 3p) \quad (2)$$

Let us assume that matter content of the Universe consists of pressure-less gas with energy density ρ_m representing baryonic plus cold dark matter (CDM) and the generalized Chaplygin gas with the equation of state

$$p_{Ch} = -\frac{A}{\rho_{Ch}^\alpha} \quad (3)$$

representing the dark energy responsible for the acceleration of the Universe. If one further makes an assumption that these two components do not interact, then the energy conservation equation

$$\dot{\rho} + 3H(\rho + p) = 0 \quad (4)$$

where $H = \dot{a}/a$ is the Hubble function, can be integrated separately for matter and Chaplygin gas leading to well known result $\rho_m = \rho_{m,0}a^{-3}$ and (see also (9))

$$\rho_{Ch} = \left(A + \frac{B}{a^{3(1+\alpha)}}\right)^{\frac{1}{1+\alpha}} \quad (5)$$

The physical interpretation of, so far arbitrary, constants A and B is the following. Adopting usual convention that current value of the scale factor a_0 is equal to 1, one can see that $\rho_{Ch,0} = (A + B)^{\frac{1}{1+\alpha}}$ represents the current energy density of the Chaplygin gas. Calculating the adiabatic speed of sound squared for the Chaplygin gas

$$c_s^2 = \frac{\partial p_{Ch}}{\partial \rho_{Ch}} = \frac{\alpha A}{\rho^{1+\alpha}} = \frac{\alpha A}{A + \frac{B}{a^{3(1+\alpha)}}}$$

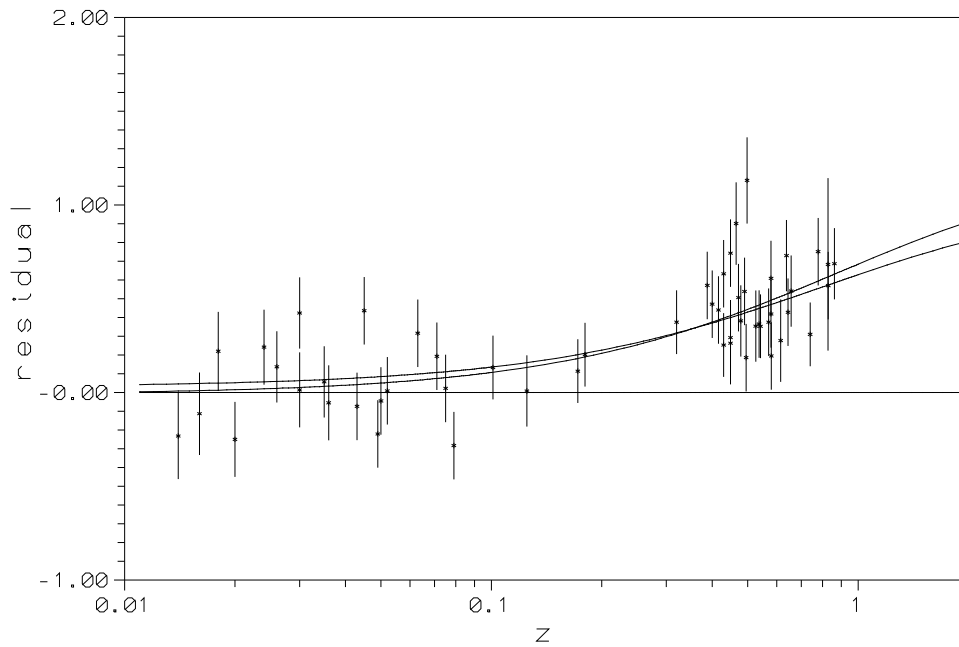


Fig. 1.— Residuals (in mag) between the Einstein-de Sitter model (zero line), the Perlmutter flat model (Λ CDM model) (upper curve) and the best-fitted Generalized Chaplygin Gas model with $\Omega_m = 0.3, \Omega_{Ch} = 0.7$ (middle curve), sample K3.

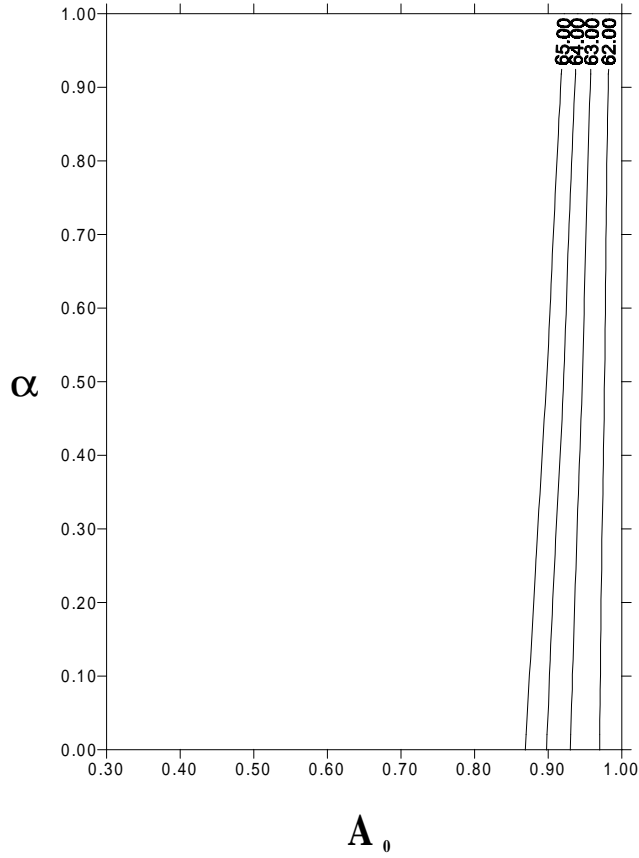


Fig. 2.— Levels of constant χ^2 on the plane (A_0, α) for Generalized Chaplygin Gas model with $\Omega_m = 0.3, \Omega_{Ch} = 0.7$, sample K3, marginalized over \mathcal{M} . The figure shows preferred values of A_0 and α .

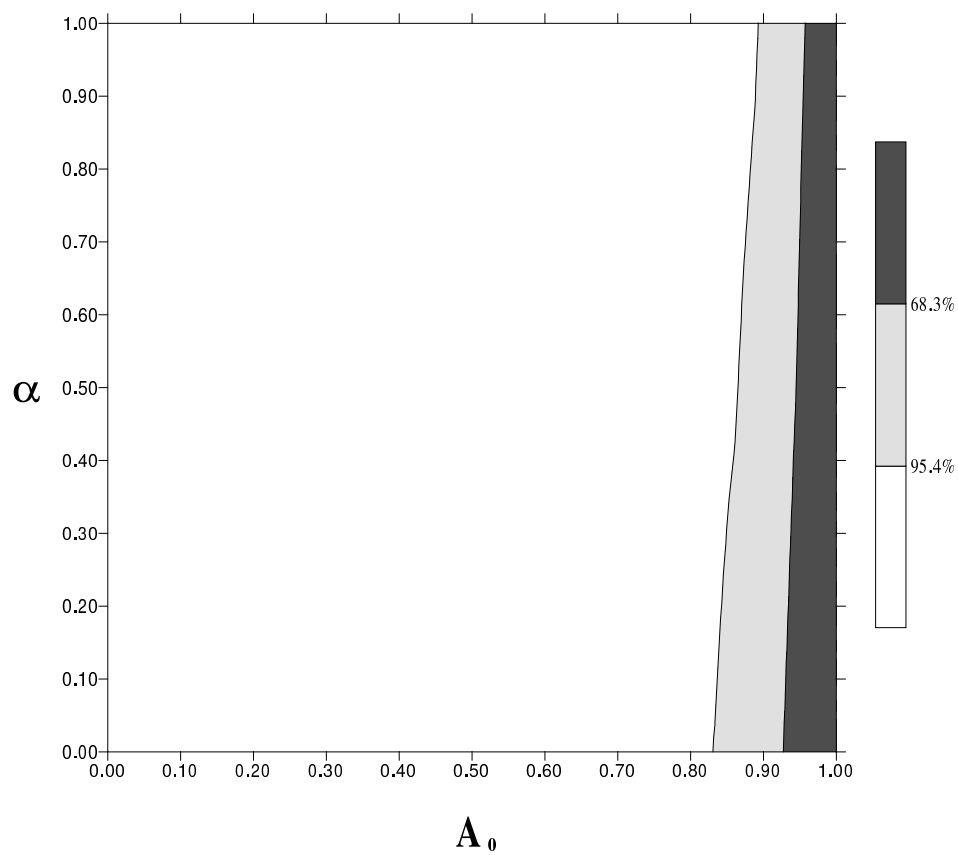


Fig. 3.— Confidence levels on the plane (A_0, α) for Generalized Chaplygin Gas model with $\Omega_m = 0.3, \Omega_{Ch} = 0.7$, sample K3, marginalized over \mathcal{M} . The figure shows the ellipses of preferred values of A_0 and α .

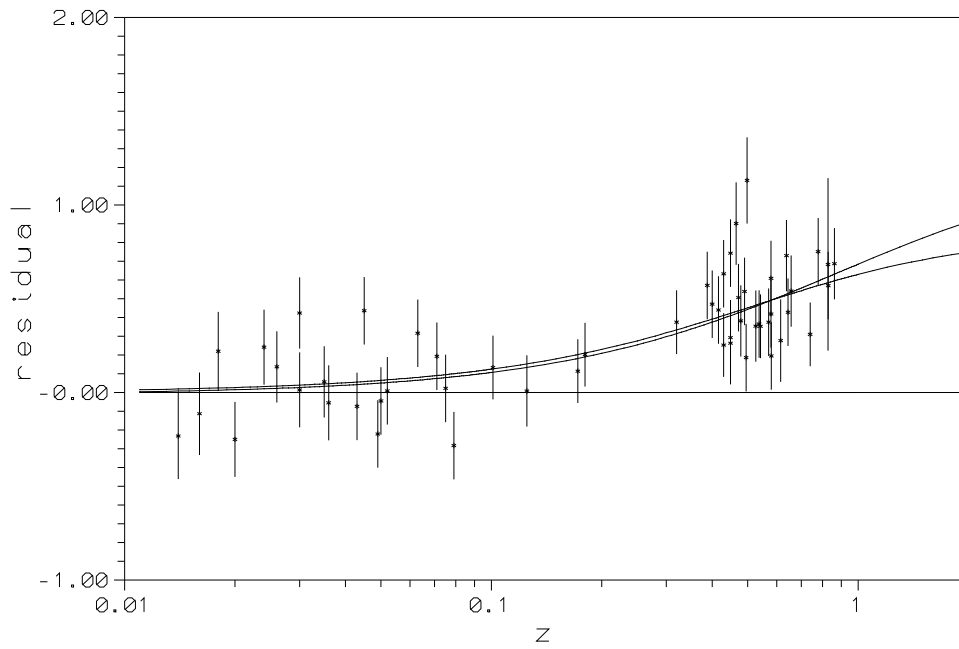


Fig. 4.— Residuals (in mag) between the Einstein-de Sitter model (zero line), the Perlmutter flat model (Λ CDM model) (upper curve) and the best-fitted Generalized Chaplygin Gas model with $\Omega_m = 0.05, \Omega_{Ch} = 0.95$ (middle curve), sample K3.

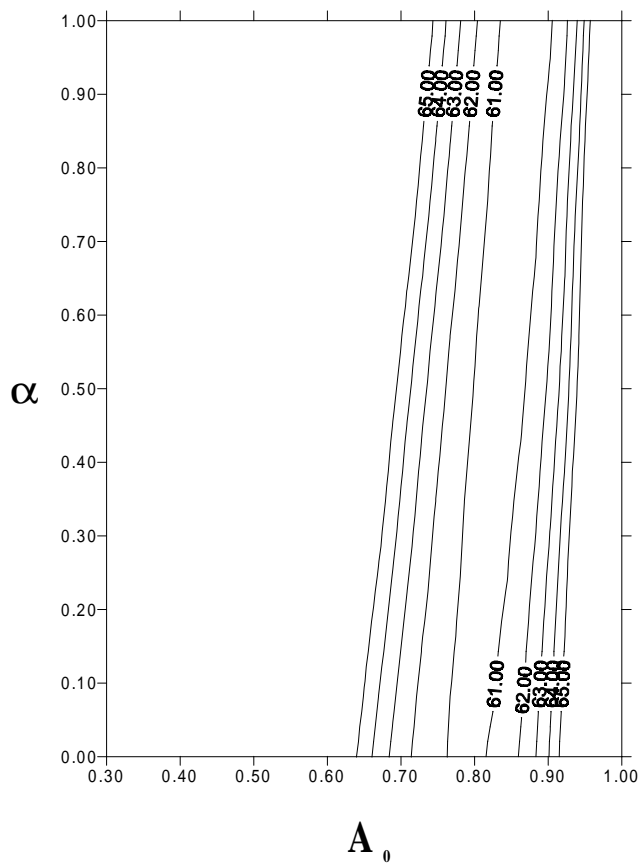


Fig. 5.— Levels of constant χ^2 on the plane (A_0, α) for Generalized Chaplygin Gas model with $\Omega_m = 0.05, \Omega_{Ch} = 0.95$, sample K3, marginalized over \mathcal{M} . The figure shows preferred values of A_0 and α .

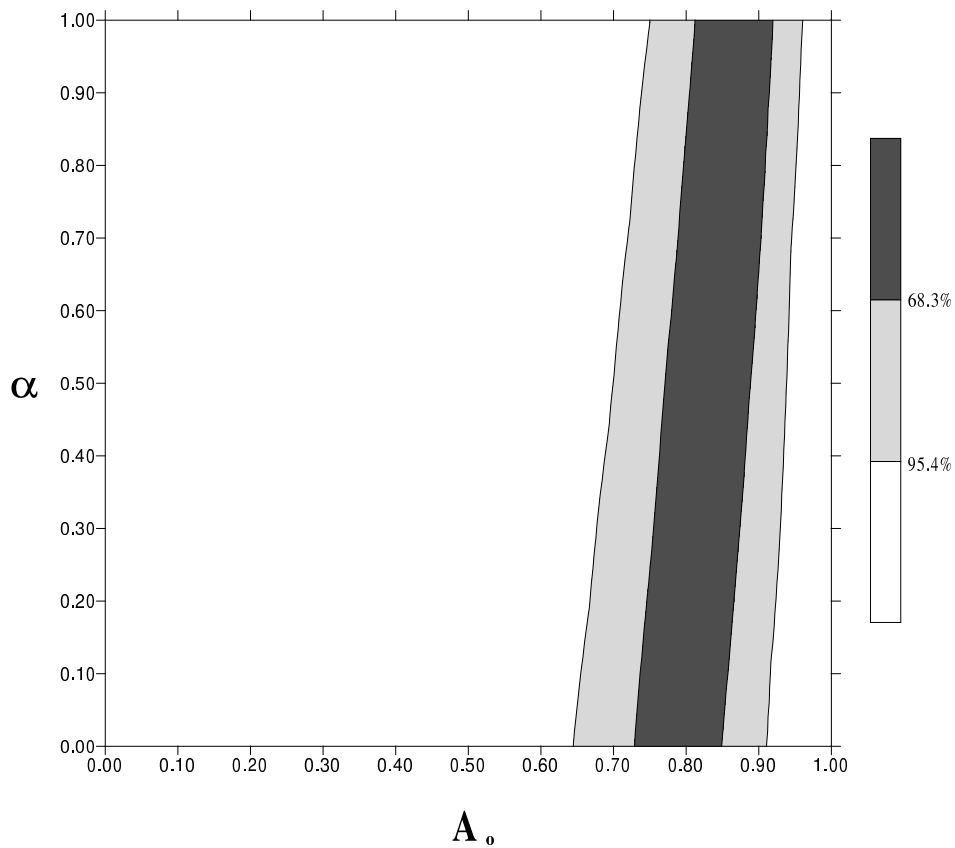


Fig. 6.— Confidence levels on the plane (A_0, α) for Generalized Chaplygin Gas model with $\Omega_m = 0.05, \Omega_{Ch} = 0.95$, sample K3, marginalized over \mathcal{M} . The figure shows the ellipses of preferred values of A_0 and α .

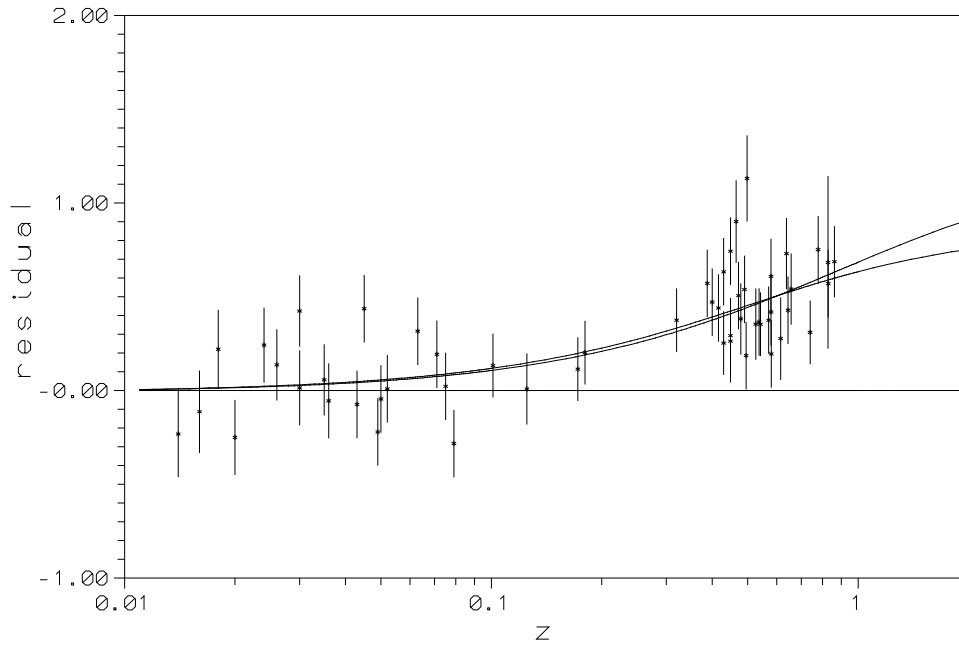


Fig. 7.— Residuals (in mag) between the Einstein-de Sitter model (zero line), the Perlmutter flat model (Λ CDM model) (upper curve) and the best-fitted Generalized Chaplygin Gas model with $\Omega_m = 0, \Omega_{Ch} = 1$ (middle curve), sample K3.

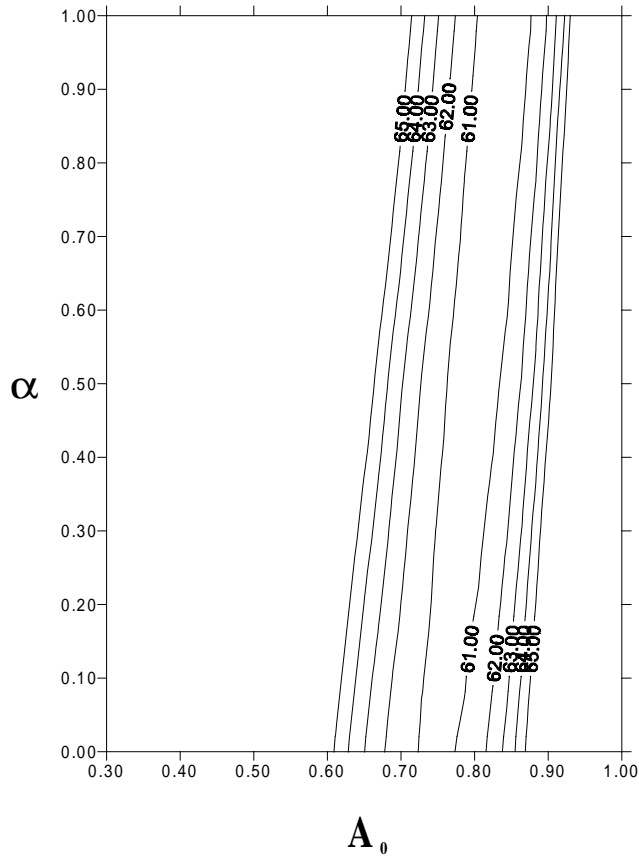


Fig. 8.— Levels of constant χ^2 on the plane (A_0, α) for Generalized Chaplygin Gas model with $\Omega_m = 0, \Omega_{Ch} = 1$, sample K3, marginalized over \mathcal{M} . The figure shows preferred values of A_0 and α .

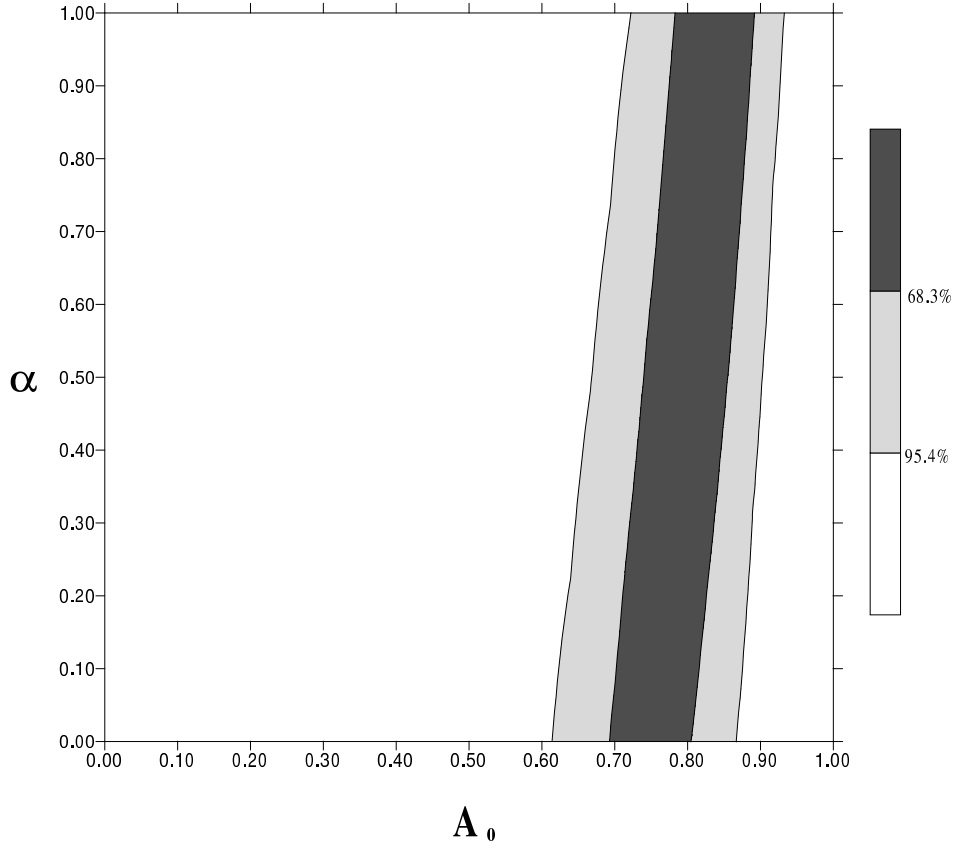


Fig. 9.— Confidence levels on the plane (A_0, α) for Generalized Chaplygin Gas model with $\Omega_m = 0, \Omega_{Ch} = 1$, sample K3, marginalized over \mathcal{M} . The figure shows the ellipses of preferred values of A_0 and α .

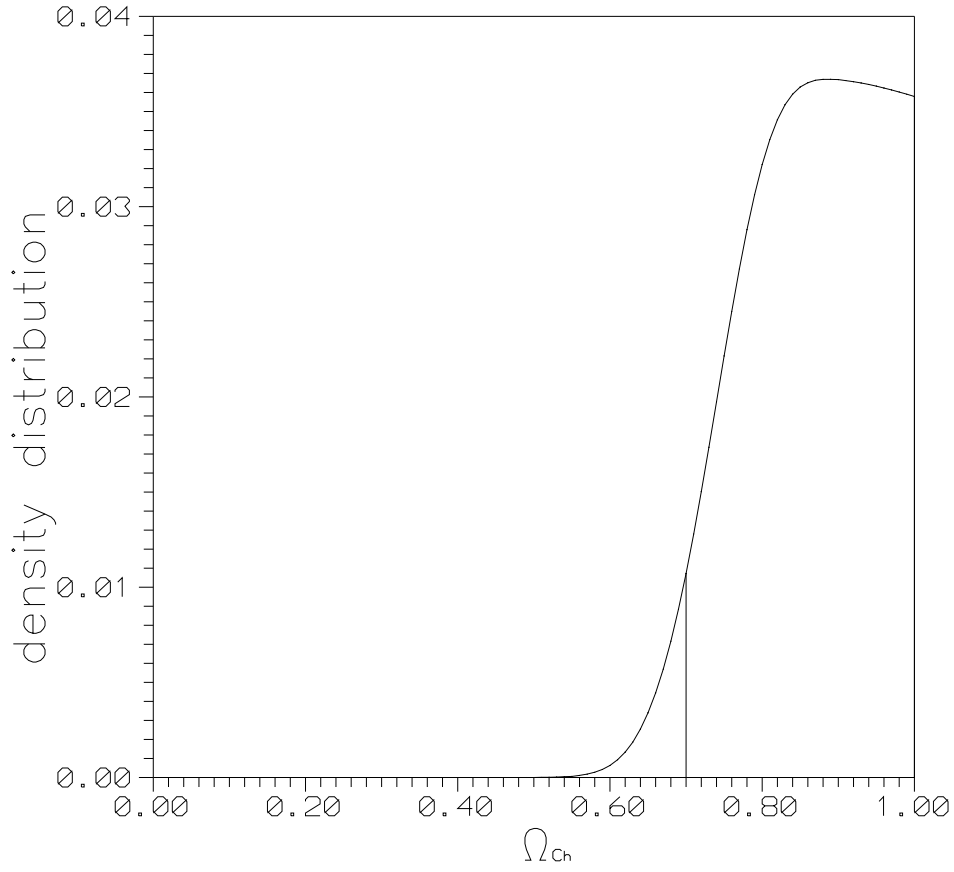


Fig. 10.— The density distribution (one dimensional PDF) for Ω_{Ch} obtained from sample K3 by marginalization over remaining parameters of the model. We obtain the limit $\Omega_{Ch} > 0.70$ at the confidence level 95.4.

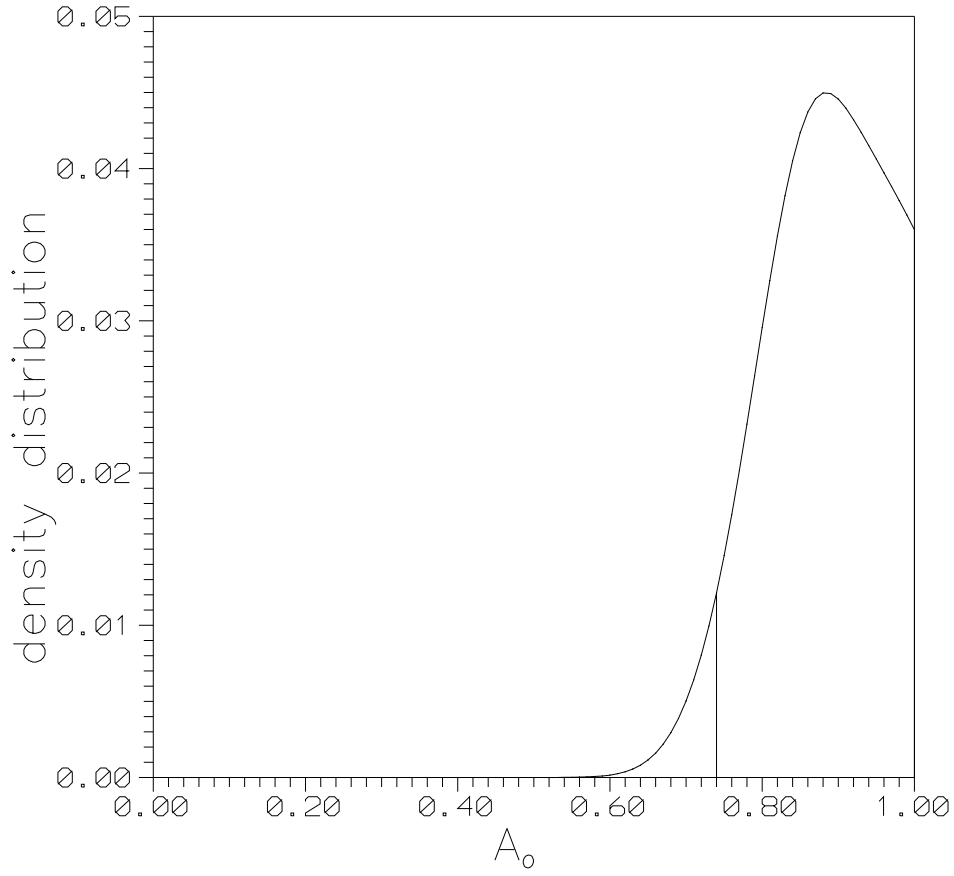


Fig. 11.— The density distribution (one dimensional PDF) for A_0 obtained from sample K3 by marginalization over remaining parameters of the model. We obtain the limit $A_0 > 0.74$ at the confidence level 95.4.

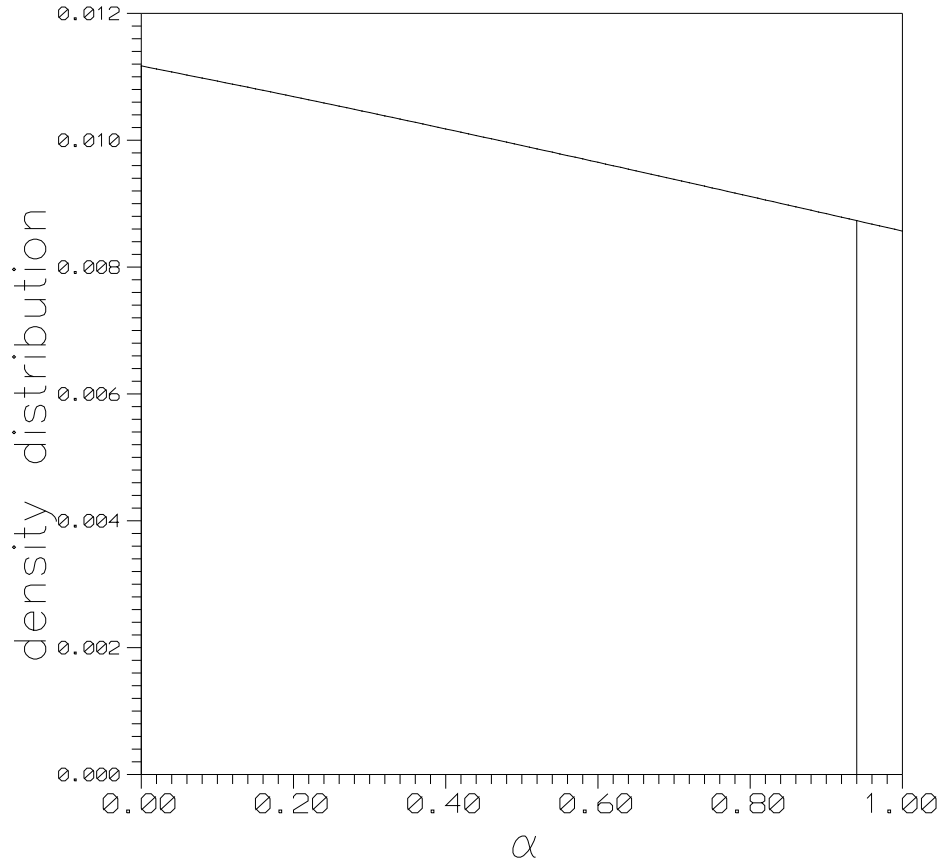


Fig. 12.— The density distribution (one dimensional PDF) for α obtained from sample K3 by marginalization over remaining parameters of the model. We obtain the limit $\alpha < 0.94$ at the confidence level 95.4 .

it is easy to confirm that the current value of c_s^2 is equal to $c_{s,0}^2 = \frac{\alpha A}{A+B}$. Hence the constants A and B can be expressed as combinations of quantities having well defined physical meaning.

Our further task will be to confront the Chaplygin gas model with SNIa data and for this purpose we have to calculate the luminosity distance in our model

$$d_L(z) = (1+z) \frac{c}{H_0} \frac{1}{\sqrt{|\Omega_k|}} \mathcal{F} \left(H_0 \sqrt{|\Omega_k|} \int_0^z \frac{dz'}{H(z')} \right) \quad (6)$$

where $\Omega_k = -\frac{k}{H_0^2}$ and

$$\mathcal{F}(x) = \sinh(x) \quad \text{for} \quad k < 0 \quad (7)$$

$$\mathcal{F}(x) = x \quad \text{for} \quad k = 0 \quad (8)$$

$$\mathcal{F}(x) = \sin(x) \quad \text{for} \quad k > 0 \quad (9)$$

The Friedman equation (1) can be rearranged to the form giving explicitly the Hubble function $H(z) = \dot{a}/a$

$$H(z)^2 = H_0^2 \left[\Omega_m (1+z)^3 + \Omega_{Ch} (A_0 + (1-A_0)(1+z)^{3(1+\alpha)})^{\frac{1}{1+\alpha}} + \Omega_k (1+z)^2 \right] \quad (10)$$

where the quantities Ω_i , $i = m, Ch, k$ represent fractions of critical density currently contained in energy densities of respective components and $\Omega_m + \Omega_{Ch} + \Omega_k = 1$. For the transparency of further formulae we have also denoted $A_0 = A/(A+B)$.

Finally the luminosity distance reads:

$$d_L(z) = (1+z) \frac{c}{H_0} \frac{1}{\sqrt{|\Omega_k|}} \mathcal{F} \left(\sqrt{|\Omega_k|} \int_0^z \frac{dz'}{\sqrt{\Omega_m (1+z)^3 + \Omega_{Ch} (A_0 + (1-A_0)(1+z)^{3(1+\alpha)})^{\frac{1}{1+\alpha}} + \Omega_k (1+z)^2}} \right) \quad (11)$$

The formula (11) is the most general one in the framework of Friedman-Robertson-Walker cosmology with generalized Chaplygin gas. Further in this paper we will use its version restricted to flat model $k = 0$ since the evidence for this case is very strong in the light of current CMBR data. Therefore while talking about model testing we actually mean the estimation of α and A_0 parameters for the best fitted flat FRW cosmological model filled with generalized Chaplygin gas.

To proceed with fitting the SNIa data we need the magnitude-redshift relation

$$m(z, \mathcal{M}, \Omega_m, \Omega_{Ch}; A_0, \alpha) = \mathcal{M} + 5 \log_{10} D_L(z, \Omega_m, \Omega_{Ch}; A_0, \alpha) \quad (12)$$

where:

$$D_L(z, \Omega_m, \Omega_{Ch}; A_0, \alpha) = H_0 d_L(z, H_0, \Omega_m, \Omega_{Ch}; A_0, \alpha)$$

is the luminosity distance with H_0 factored out so that marginalization over the intercept

$$\mathcal{M} = M - 5 \log_{10} H_0 + 25 \quad (13)$$

leads actually to joint marginalization over H_0 and M (M being the absolute magnitude of SNIa).

Then we can obtain the best fit model minimalizing the χ^2 function

$$\chi^2 = \sum_i \frac{(m_i^{Ch} - m_i^{obs})^2}{\sigma_i^2}$$

where the sum is over the SNIa sample and σ_i denote the (full) statistical error of magnitude determination. This is illustrated by figures of residuals (with respect to Einstein-de Sitter model) and χ^2 levels in the (A_0, α) plane. One of the advantages of residual plots is that the intercept of the $m - z$ curve gets cancelled. The assumption that the intercept is the same for different cosmological models is legitimate since \mathcal{M} is actually determined from the low-redshift part of the Hubble diagram which should be linear in all realistic cosmologies. From the full sample (see below) we have obtained $\mathcal{M} = -3.39$ which is in a very good agreement with the values reported in the literature (1).

However, the best-fit values alone are not relevant if not supplemented with the confidence levels for the parameters. Therefore, we performed the estimation of model parameters using the minimization procedure, based on the likelihood function. We assumed that supernovae measurements came with uncorrelated Gaussian errors and in this case the likelihood function \mathcal{L} could be determined from chi-square statistic $\mathcal{L} \propto \exp(-\chi^2/2)$ (1).

Therefore we supplement our analysis with confidence intervals in the (A_0, α) plane by calculating the marginal probability density functions

$$\mathcal{P}(A_0, \alpha) \propto \int \exp(-\chi^2(\Omega_m, \Omega_{Ch}, A_0, \alpha, \mathcal{M})/2) d\mathcal{M}$$

with Ω_m, Ω_{Ch} fixed ($\Omega_m = 0.0, 0.05, 0.3$) and

$$\mathcal{P}(A_0, \alpha) \propto \int \exp(-\chi^2(\Omega_m, \Omega_{Ch}, A_0, \alpha, \mathcal{M})/2) d\Omega_m$$

with \mathcal{M} fixed ($\mathcal{M} = -3.39$) respectively (proportionality sign means equal up to the normalization constant). In order to complete the picture we have also derived one-dimensional probability distribution functions for Ω_{Ch} obtained from joint marginalization over α and A_0 . The maximum value of such PDF informs us about the most probable value of Ω_{Ch} (supported by supernovae data) within the full class of generalized Chaplygin gas models.

Table 1. Results of statistical analysis of Generalized Chaplygin Gas model (with marginalization over \mathcal{M}) performed on analysed samples of SNIA (A, C, K3, K6 TBI, TBII) as a minimum χ^2 best-fit (denoted BF) and with the maximum likelihood method (denoted L) with no prior on Ω_m (first two rows for each sample). The same analysis was repeated with fixed $\Omega_m = 0.0$, $\Omega_m = 0.05$ and $\Omega_m = 0.3$.

sample	Ω_m	Ω_{Ch}	A_0	α	\mathcal{M}	χ^2	method
A	0.00	1.00	0.77	1.00	-3.39	95.4	BF
	0.17	0.83	0.83	0.00	-3.36	—	L
	0.00	1.00	0.77	1.00	-3.39	95.4	BF
	0.00	1.00	0.73	1.00	-3.38	—	L
	0.05	0.95	0.80	1.00	-3.39	95.4	BF
	0.05	0.95	0.76	1.00	-3.38	—	L
	0.30	0.70	0.96	1.00	-3.39	95.8	BF
	0.30	0.70	0.96	0.00	-3.38	—	L
C	0.00	1.00	0.80	1.00	-3.44	52.9	BF
	0.15	0.85	0.86	0.00	-3.41	—	L
	0.00	1.00	0.80	1.00	-3.44	52.9	BF
	0.00	1.00	0.76	0.49	-3.43	—	L
	0.05	0.95	0.83	1.00	-3.44	53.0	BF
	0.05	0.95	0.79	0.11	-3.43	—	L
	0.30	0.70	0.99	1.00	-3.42	53.3	BF
	0.30	0.70	0.99	0.00	-3.39	—	L
K6	0.00	1.00	0.81	1.00	-3.52	55.3	BF
	0.10	0.90	0.88	0.00	-3.51	—	L
	0.00	1.00	0.81	1.00	-3.52	55.3	BF
	0.00	1.00	0.78	0.71	-3.52	—	L
	0.05	0.95	0.84	1.00	-3.52	55.4	BF
	0.05	0.95	0.81	0.06	-3.52	—	L
	0.30	0.70	1.00	1.00	-3.51	55.9	BF
	0.30	0.70	1.00	0.00	-3.49	—	L
K3	0.00	1.00	0.85	1.00	-3.48	60.4	BF
	0.11	0.89	0.88	0.00	-3.45	—	L
	0.00	1.00	0.85	1.00	-3.48	60.4	BF
	0.00	1.00	0.80	0.30	-3.47	—	L
	0.05	0.95	0.87	1.00	-3.47	60.4	BF
	0.05	0.95	0.84	0.00	-3.47	—	L
	0.30	0.70	1.00	1.00	-3.44	61.4	BF
	0.30	0.70	0.96	0.00	-3.42	—	L
TBI	0.00	1.00	0.79	1.00	15.895	273.9	BF
	0.00	1.00	0.81	1.00	15.905	—	L
	0.00	1.00	0.79	1.00	15.895	273.8	BF
	0.00	1.00	0.75	1.00	15.905	—	L
	0.05	0.95	0.82	1.00	15.895	274.0	BF
	0.05	0.95	0.78	1.00	15.915	—	L
	0.30	0.70	0.97	1.00	15.915	275.8	BF
	0.30	0.70	0.98	0.00	15.915	—	L
TBII	0.00	1.00	0.78	1.00	15.915	186.5	BF
	0.00	1.00	0.81	1.00	15.925	—	L
	0.00	1.00	0.78	1.00	15.915	186.5	BF
	0.00	1.00	0.75	1.00	15.915	—	L
	0.05	0.95	0.81	1.00	15.915	186.6	BF
	0.05	0.95	0.78	1.00	15.925	—	L

3. Fits to A_0 and α parameters

Samples from the original Perlmutter data (1) chosen for the analysis comprise the full sample reported by Perlmutter (sample A) and a sub-sample after excluding two outliers differing the most from the average lightcurve and two outliers claimed to be likely reddened (sample C).

The Perlmutter data were gathered four years ago, hence it would be interesting to use more recent supernovae data as well. Recently Knop et al. (10) have reexamined the Perlmutter’s data with host-galaxy extinction correctly assessed. From the Perlmutter’s sample they chose only these supernovae which were spectroscopically safely identified as type Ia and had reasonable color measurements. They also included eleven new high redshift supernovae and a well known sample with low redshift supernovae.

In (10) a few subsamples have been distinguished. We consider two of them. The first is a subset of 58 supernovae with corrected extinction (Knop subsample 6; hereafter K6) and the second is that of 54 low extinction supernovae (Knop subsample 3; hereafter K3). Samples C and K3 are similarly constructed as containing only low extinction supernovae.

On these samples we have tested Generalized Chaplygin gas cosmology in three different classes of models with (1) $\Omega_m = 0.3$, $\Omega_{Ch} = 0.7$; (2) $\Omega_m = 0.05$, $\Omega_{Ch} = 0.95$ and (3) $\Omega_m = 0$, $\Omega_{Ch} = 1$. We started with a fixed value of $\mathcal{M} = -3.39$.

The first class was chosen as representative of the standard knowledge of Ω_m (baryonic plus dark matter in galactic halos (11)) with Chaplygin gas responsible for the missing part of closure density (the dark energy). Best fit (with fixed value of $\mathcal{M} = -3.39$) from the sample A is ($\alpha = 1$, $A_0 = 0.96$) at the $\chi^2 = 95.8$. Sample C gives the best fit of ($\alpha = 0.95$, $A_0 = 0.95$) at the $\chi^2 = 53.6$.

In the second class we have incorporated (at the level of Ω_m) the prior knowledge about baryonic content of the Universe (as inferred from the BBN considerations). Hence this class is representative of the models in which Chaplygin gas is allowed to clump and is responsible both for dark matter in halos as well as its diffuse part (dark energy). Sample A gives the best fit of ($\alpha = 1$, $A_0 = 0.80$) at the $\chi^2 = 95.4$ whereas the sample C gives the best fit

Table 1—Continued

sample	Ω_m	Ω_{Ch}	A_0	α	\mathcal{M}	χ^2	method
	0.30	0.70	0.97	1.00	15.925	188.4	BF
	0.30	0.70	0.96	0.00	15.935	—	L

Table 2: Generalized Chaplygin gas model parameter values obtained from the marginal probability density functions calculated on Perlmutter and Knop samples.

sample	Ω_m	Ω_{Ch}	A_0	α
A	$0.17^{+0.08}_{-0.17}$	$0.83^{+0.17}_{-0.08}$	$0.83^{+0.14}_{-0.09}$	$-0.0^{+0.67}$
C	$0.15^{+0.08}_{-0.15}$	$0.85^{+0.15}_{-0.08}$	$0.86^{+0.13}_{-0.10}$	$0.0^{+0.66}$
K6	$0.10^{+0.11}_{-0.10}$	$0.90^{+0.10}_{-0.11}$	$0.88^{+0.12}_{-0.08}$	$-0.0^{+0.66}$
K3	$0.11^{+0.07}_{-0.11}$	$0.89^{+0.11}_{-0.07}$	$0.88^{+0.11}_{-0.05}$	$0.0^{+0.66}$
TBI	$0.00^{+0.21}$	$1.00_{-0.21}$	$0.81^{+0.12}_{-0.07}$	$1.0_{-0.60}$
TBII	$0.00^{+0.21}$	$1.00_{-0.21}$	$0.81^{+0.12}_{-0.07}$	$1.0_{-0.62}$

Table 3: Results of statistical analysis of Generalized Chaplygin Gas non-flat model (with marginalization over \mathcal{M}) performed Knop Samples K3 as a minimum χ^2 best-fit (denoted BF) and with the maximum likelihood method (denoted L) with no prior on Ω_m (first two rows). The same analysis was repeated with fixed $\Omega_m = 0.0$, $\Omega_m = 0.05$ and $\Omega_m = 0.3$.

sample	Ω_k	Ω_m	Ω_{Ch}	A_0	α	\mathcal{M}	χ^2	method
K3	-0.19	0.00	1.19	0.82	1.00	-3.48	60.3	BF
	-0.60	0.00	1.26	0.89	0.00	-3.46	—	L
	-0.25	0.00	1.25	0.82	1.00	-3.49	60.3	BF
	0.10	0.00	0.90	0.76	0.00	-3.46	—	L
	-0.28	0.05	1.23	0.84	1.00	-3.49	60.3	BF
	0.05	0.05	0.90	0.78	0.00	-3.47	—	L
	-0.48	0.30	1.18	0.93	0.97	-3.49	60.3	BF
	-0.35	0.30	1.05	0.88	0.00	-3.47	—	L

($\alpha = 0.51, A_0 = 0.73$) at the $\chi^2 = 53.7$.

Finally, the third class is a kind of toy model – the FRW Universe filled completely with Chaplygin gas. We have considered it mainly in order to see how sensitive the SNIa test is with respect to parameters identifying the cosmological model. Again the sample A gives the best fit of ($\alpha = 1, A_0 = 0.77$) at the $\chi^2 = 95.4$ whereas the sample C gives the best fit ($\alpha = 0.42, A_0 = 0.69$) at the $\chi^2 = 53.7$.

It should be noted, however that the fitting procedure for sample C prefers $\mathcal{M} = -3.44$ instead of $\mathcal{M} = -3.39$ as for sample A. If one takes this value the results for sample C will change respectively and then for the first class $A_0 = 1$ (at $\chi^2 = 53.5$) what means (see equation (10)) that α can be arbitrary and the problem is effectively equivalent to the model with cosmological constant. Analogously, for the second class $A_0 = 0.83 \alpha = 1$ (at $\chi^2 = 52.9$), while for third class $A_0 = 0.80 \alpha = 1$ (at $\chi^2 = 52.9$). This indicates clearly that model parameters, especially α strongly depend on the choice of \mathcal{M} .

Separately we analyzed the data without any prior assumption about Ω_m . For the sample A we obtain as a best fit (minimizing χ^2) $\Omega_m = 0.$, ($\alpha = 1, A_0 = 0.77$) at the $\chi^2 = 95.4$. For sample C assuming $\mathcal{M} = -3.39$ we obtain $\Omega_m = 0.27$, ($\alpha = 1, A_0 = 0.93$) with $\chi^2 = 53.6$ while for $\mathcal{M} = -3.44$ the best fit gives $\Omega_m = 0.$, ($\alpha = 1, A_0 = 0.80$) with $\chi^2 = 52.9$.

Joint marginalization over A_0 and α gives the following results. For the sample A we obtain $\Omega_{Ch} = 0.82$ (hence $\Omega_m = 0.18$), with the limit $\Omega_{Ch} \geq 0.76$ at the confidence level 68.3% and $\Omega_{Ch} \geq 0.69$ at the confidence level 95.4%. For the sample C we obtain (for $\mathcal{M} = -3.39$) $\Omega_{Ch} = 0.76$ (hence $\Omega_m = 0.24$), with the limit $\Omega_{Ch} \in (0.69, 0.94)$ on the confidence level 68.3% and $\Omega_{Ch} \geq 0.62$ at the confidence level 95.4%. For $\mathcal{M} = -3.44$ we obtain: $\Omega_{Ch} = 0.84$ (hence $\Omega_m = 0.16$), with the limit $\Omega_{Ch} \in (0.79, 0.98)$ on the confidence level 68.3% and $\Omega_{Ch} \geq 0.69$ at the confidence level 95.4%.

One could see that results are different for different values of the intercept \mathcal{M} in each sample. Therefore we additionally analyzed our samples marginalized over \mathcal{M} . The results are displayed in Table 1. First rows for each sample correspond to no prior on Ω_m assumed. Two fitting procedures were used: χ^2 fitting (denoted as BF) and maximum likelihood method (denoted L). For sample A we obtain $\Omega_{Ch} = 0.83$ (hence $\Omega_m = 0.17$), with the limit $\Omega_{Ch} \geq 0.75$ at the confidence level 68.3% while for sample C we obtain $\Omega_{Ch} = 0.85$ (hence $\Omega_m = 0.15$), with the limit $\Omega_{Ch} \geq 0.77$ at the confidence level 68.3%.

With the marginalization procedure we can also obtain one dimensional probability distribution function (PDF) for A_0 and α . For the sample A we obtain the following results. In the class (1) models ($\alpha = 0, A_0 = 0.96$) with the limit $\alpha \in (0, 0.65)$ and $A_0 \in (0.87, 1)$ at

the confidence level 68.3% and $\alpha\epsilon(0, 0.95)$ and $A_0\epsilon(0.75, 1.)$ at the confidence level 95.4% In the class (2) models ($\alpha = 1, A_0 = 0.76$ with the limit $\alpha\epsilon(0.34, 1.)$ and $A_0\epsilon(0.67, 0.84)$ at the confidence level 68.3% and $\alpha\epsilon(0.05, 1)$ and $A_0\epsilon(0.57, 0.91)$ at the confidence level 95.4%. And in the class (3) models ($\alpha = 1.0, A_0 = 0.73$) with the limit $\alpha\epsilon(0.37, 1.)$ and $A_0\epsilon(0.63, 0.81)$ at the confidence level 68.3% and $\alpha\epsilon(0.04, 1.)$ and $A_0\epsilon(0.54, 0.88)$ at the confidence level 95.4%

For the sample C we obtain: in the class (1) models ($\alpha = 0, A_0 = 0.99$) with the limit $\alpha\epsilon(0, 0.64)$ and $A_0\epsilon(0.88, 1)$ at the confidence level 68.3% and $\alpha\epsilon(0, 0.95)$ and $A_0\epsilon(0.73, 1.)$ at the confidence level 95.4%. In the class (2) models ($\alpha = 0.11, A_0 = 0.79$) with the limit $\alpha\epsilon(0, 0.68)$ and $A_0\epsilon(0.68, 0.87)$ at the confidence level 68.3% and $\alpha\epsilon(0, 0.96)$ and $A_0\epsilon(0.57, 0.94)$ at the confidence level 95.4%. And in the class (3) models ($\alpha = 0.49, A_0 = 0.76$) with the limit $\alpha\epsilon(0.14, 0.85)$ and $A_0\epsilon(0.66, 0.84)$ at the confidence level 68.3% and $\alpha\epsilon(0.03, 0.98)$ and $A_0\epsilon(0.54, 0.90)$ at the confidence level 95.4% The results for Knop sample K3 are summarized in Figures 10-12. Table 2 contains the results of joint marginalization over Ω_m, A_0 and α .

One can see from the Table 1 that working on Knop samples had not influenced the conclusions in a significant way. However the errors of parameter estimation decreased noticeably (see Table 2).

For example for the sample K3 we obtain: in the class (1) models ($\alpha = 0, A_0 = 1.00$) with the limit $\alpha\epsilon(0, 0.63)$ and $A_0\epsilon(0.94, 1)$ at the confidence level 68.3% and $\alpha\epsilon(0, 0.94)$ and $A_0\epsilon(0.86, 1.)$ at the confidence level 95.4%. In the class (2) models ($\alpha = 0., A_0 = 0.84$) with the limit $\alpha\epsilon(0, 0.67)$ and $A_0\epsilon(0.69, 0.94)$ at the confidence level 68.3% and $\alpha\epsilon(0, 0.96)$ and $A_0\epsilon(0.77, 0.89)$ at the confidence level 95.4%. And in the class (3) models ($\alpha = 0.30, A_0 = 0.80$) with the limit $\alpha\epsilon(0.00, 0.69)$ and $A_0\epsilon(0.74, 0.86)$ at the confidence level 68.3% and $\alpha\epsilon(0.00, 0.96)$ and $A_0\epsilon(0.66, 0.91)$ at the confidence level 95.4%

The above mentioned results for the Knopp sample K3 are illustrated on figures Fig. 1 - 17.

In Fig. 1 we present residual plots of redshift-magnitude relations between the Einstein-de Sitter model (represented by zero line) the best-fitted Generalized Chaplygin Gas model with $\Omega_m = 0.3, \Omega_{Ch} = 0.7$ (middle curve) and the Perlmutter flat model (Λ CDM model with $\Lambda = 0.75$ and $\Omega_m = 0.25$ (10)) – upper curve. One can observe that systematic deviation between Λ CDM model and Generalized Chaplygin Gas model gets larger at higher redshifts.

Levels of constant χ^2 on the (A_0, α) plane for Generalized Chaplygin Gas model with $\Omega_m = 0.3, \Omega_{Ch} = 0.7$, marginalized over \mathcal{M} are presented in Figure 2. The figure shows preferred values of A_0 and α . Figure 3 displays confidence levels on the (A_0, α) plane for Generalized Chaplygin Gas model with $\Omega_m = 0.3, \Omega_{Ch} = 0.7$, marginalized over \mathcal{M} . This figure shows the ellipses of preferred values of $(A_0$ and $\alpha)$.

Similar results for the models with $\Omega_m = 0.05, \Omega_{Ch} = 0.95$ and $\Omega_m = 0, \Omega_{Ch} = 1$ are presented in the figures 4 - 9 respectively.

Separately we repeated our analysis without prior assumptions on Ω_m . The density distribution (one dimensional PDF) for model parameters obtained by marginalization over remaining parameters of the model are presented in Figures 10-12.

Residuals (in mag) between the Einstein-de Sitter model (zero line), Perlmutter flat model (Λ CDM model) – upper curve – and the best-fitted Generalized Chaplygin Gas model (without prior assumptions on Ω_m) – middle curve – are presented on Figure 13, while levels of constant χ^2 and confidence levels on the (A_0, α) plane (marginalized over \mathcal{M}) are presented on Figs. 14 and 15.

One should notice that as a best fit we obtain $\Omega_m = 0, \Omega_{Ch} = 1, A_0 = 0.85, \alpha = 1$ i.e. results are the same as for a toy model with Chaplygin gas only ($\Omega_{Ch} = 1$). One could note, that formally we could also analysed models with $\alpha > 1$. However, due to large error in estimation of value of the α parameter, it is no reason to analyse such possibilities, with the present supernovae data.

Levels of constant χ^2 on the (Ω_m, α) plane for Generalized Chaplygin Gas model, marginalized over \mathcal{M} and A_0 are presented on Figure 16, while confidence levels on the (Ω_m, α) plane (marginalized over \mathcal{M} , and A_0) are presented on Figure 17. This figure shows that all three model with $\Omega_{Ch} = 1, \Omega_{Ch} = 0.95$, and $\Omega_{Ch} = 0.7$, are statistically admissible by current Supernovae data.

Another sample was recently presented by Tonry *et al.* (20) who collected a large number of supernovae data published by different authors and added eight new high redshift SN Ia. This sample of 230 SNe Ia was recalibrated with a consistent zero point. Wherever it was possible the extinctions estimates and distance fitting were recalculated. Unfortunately, one was not able to do so for the full sample (for details see Table 8 in (20)). This sample was further improved by Barris who added 23 high redshift supernovae including 15 at $z \geq 0.7$ thus doubling the published record of objects at these redshifts (21). Despite of the above mentioned problems, the analysis of our model using this sample of supernovae could be interesting. Hence for comparison, we decided to repeat our analysis with the Tonry/Barris sample.

However, because Knop's discussion of extinction correction was very careful and as a result his sample has extinction correctly applied, we think that using the limit obtained from the Knop's sample is the most appropriate and we have used it as a our base sample. We decided to analyze two Tonry/Bariss subsamples. First, we considered the full Tonry/Barris sample of 253 SNe Ia (hereafter sample TBI). The sample contains 218 SNe Ia with low

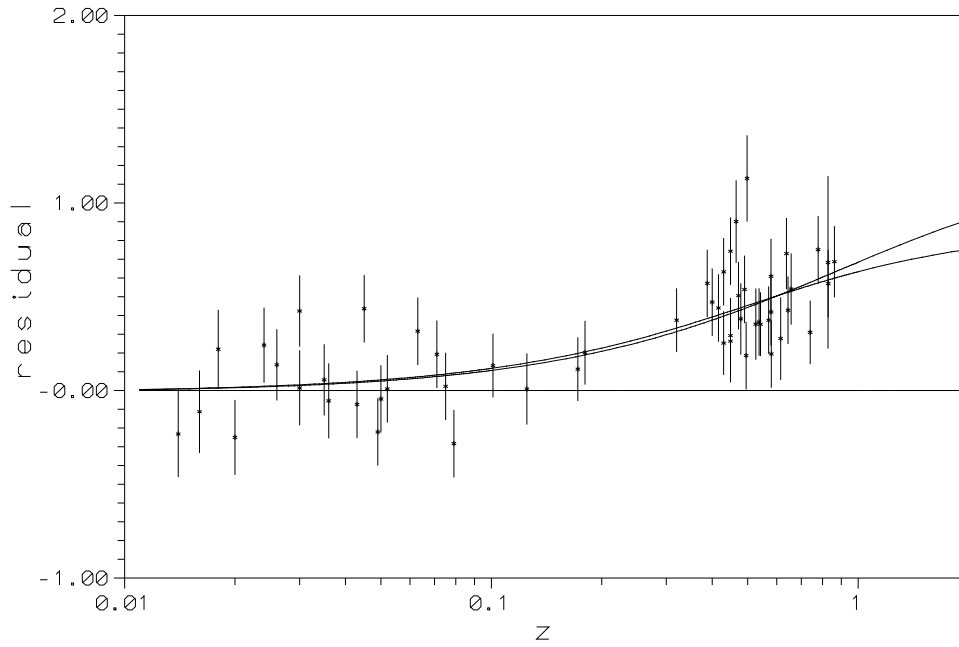


Fig. 13.— Residuals (in mag) between the Einstein-de Sitter model (zero line), the Perlmutter flat model (Λ CDM model) (upper curve) and the best-fitted Generalized Chaplygin Gas model (without any prior assumptions on Ω_m) (middle curve), sample K3.

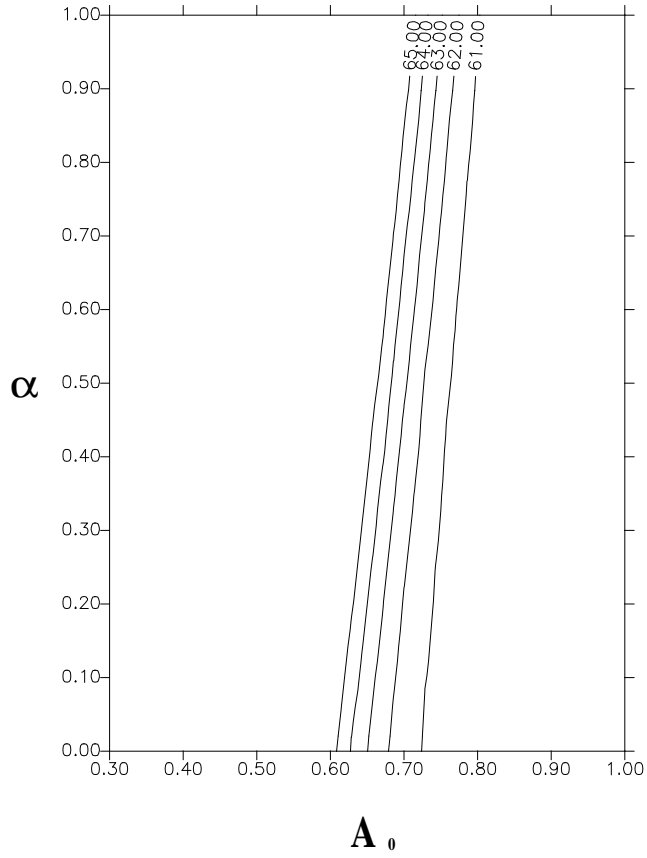


Fig. 14.— Levels of constant χ^2 on the plane (A_0, α) for Generalized Chaplygin Gas model, sample K3, marginalized over \mathcal{M} , and Ω_m . The figure shows preferred values of A_0 and α .

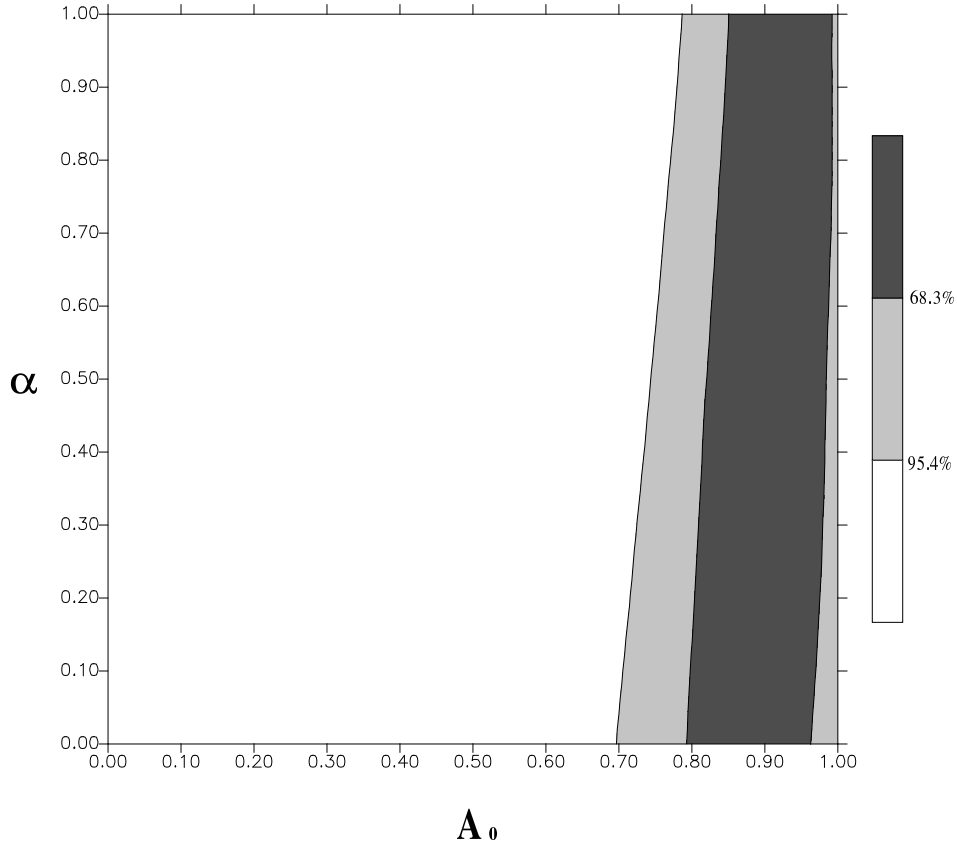


Fig. 15.— Confidence levels on the plane (A_0, α) for Generalized Chaplygin Gas model, sample K3, marginalized over \mathcal{M} , and Ω_m . The figure shows the ellipses of preferred values of A_0 and α .

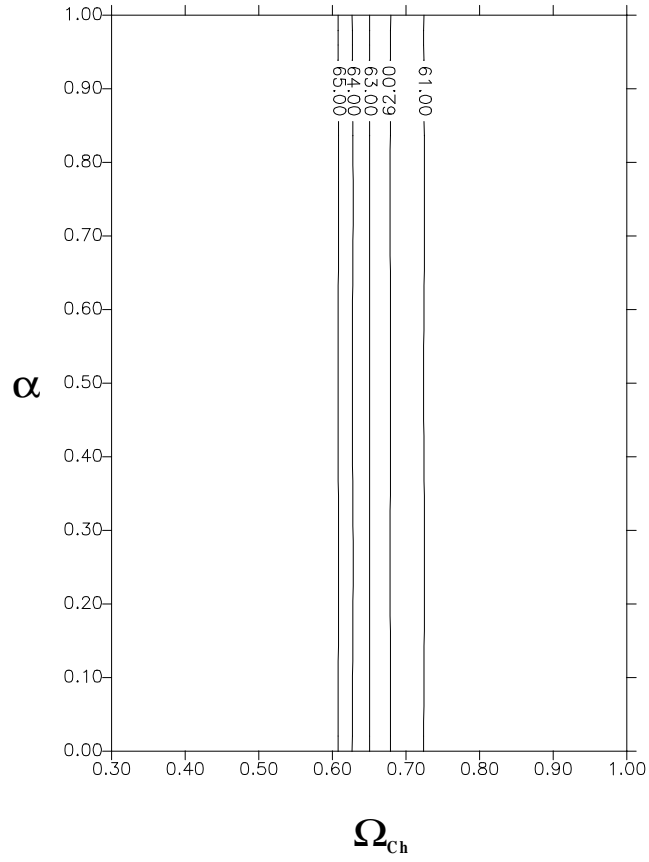


Fig. 16.— Levels of constant χ^2 on the plane (Ω_m, α) for Generalized Chaplygin Gas model, sample K3, marginalized over \mathcal{M} , and A_0 . The figure shows preferred values of Ω_m , and α .

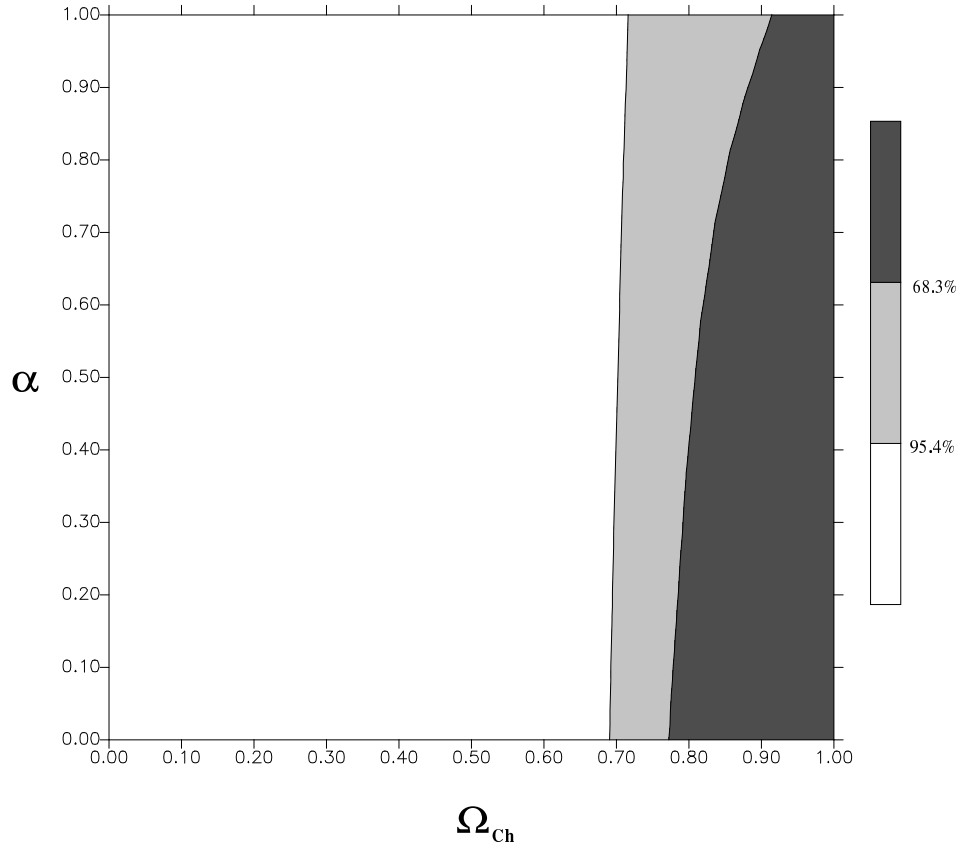


Fig. 17.— Confidence levels on the plane (Ω_m, α) for Generalized Chaplygin Gaz model, sample K3, marginalized over \mathcal{M} , and A_0 . The figure shows the ellipses of preferred values of Ω_m , and α .

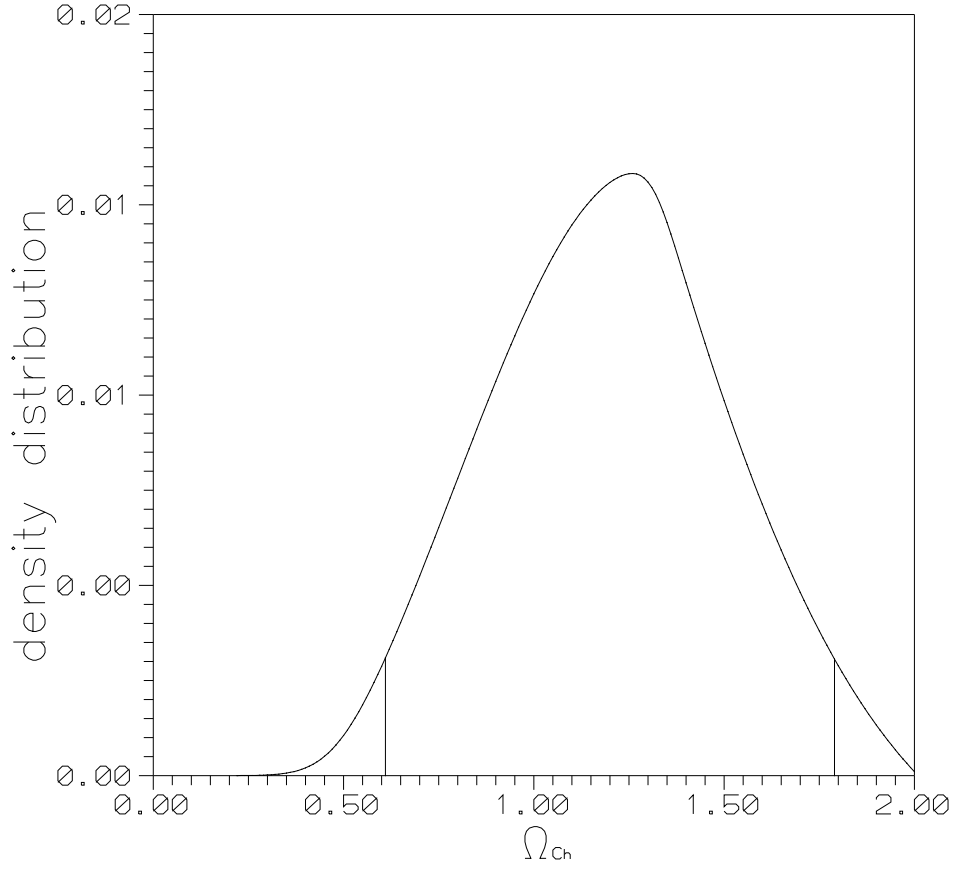


Fig. 18.— The density distribution (one dimensional PDF) for Ω_{Ch} obtained from sample K3 by marginalization over remaining parameters of the model. We obtain the limit $\Omega_{Ch} \in (0.61, 1.79)$ at the confidence level 95.4%. (NON-flat GCG model.)

extinction. Because Tonry’s sample has a lot of outliers especially in low redshift, we decided to analyse the sample where all low redshift ($z < 0.01$) supernovae were excluded. In the sample of 193 SN Ia all supernovae with low redshift and high extinction were removed (hereafter sample TBII).

Tonry and Barris (20; 21) presented the data of redshifts and luminosity distances for their supernovae sample. Therefore, Eqs. (12) and (13) should be modified appropriately (22):

$$m - M = 5 \log_{10}(\mathcal{D}_L)_{\text{Tonry}} - 5 \log_{10} 65 + 25 \quad (14)$$

and

$$\mathcal{M} = -5 \log_{10} H_0 + 25. \quad (15)$$

For the Hubble constant $H_0 = 65 \text{ km s}^{-1} \text{ Mpc}^{-1}$ one gets $\mathcal{M} = 15.935$.

The results obtained with Tonry/Bariss sample are similar to those obtained with previous samples. For example TBII sample gives the best fit: $\Omega_m = 0, \Omega_{Ch} = 1, A_0 = 0.78, \alpha = 1$ i.e. nearly the same as in the case of K3 sample.

Joint marginalization over parameters gives the following results: $\Omega_{Ch} = 1.00$ (hence $\Omega_m = 0.0$), with the limit $\Omega_{Ch} \geq 0.79$ at the confidence level of 68.3% and $\Omega_{Ch} \geq 0.67$ at the confidence level of 95.4%. ($\alpha = 1.0, A_0 = 0.73$) with the limit $\alpha \in (0.40, 1.)$ and $A_0 \in (0.74, 0.93)$ at the confidence level of 68.3% and $\alpha \in (0.06, 1.)$ and $A_0 \in (0.70, 1.00)$ at the confidence level of 95.4%. One can see that errors in the case of Tonry/Bariss sample are larger than in the case of Knop’s sample. It supports our choice of using Knop’s sample as a baseline.

Then we extended our analysis on Knop’s sample by adding a curvature term to the original GCG model. Then in equation (10) we must take into account the Ω_k term. For statistical analysis we restricted the values of the Ω_m parameter to the interval $[0, 1]$, Ω_{Ch} to the interval $[0, 2]$ and Ω_k was obtained from the constraint $\Omega_m + \Omega_{Ch} + \Omega_k = 1$. However, the cases $\Omega_k < -1$ were excluded from the analysis. The results are presented in Table III.

In the model without prior assumptions on Ω_m we obtain $\Omega_k = -0.19$ as a best fit, while with maximum likelihood method prefers $\Omega_k = -0.60$.

However, the model with priors on Ω_m or Ω_{Ch} the maximum likelihood method prefers the universe much “closer” to the flat one. Specifically, for the ”toy” model with Chaplygin Gas only one gets $\Omega_k = 0.10$ and $\Omega_k = 0.05$ for the model with baryonic content only $\Omega_m = 0.05$. One should emphasize that even though we allowed $\Omega_k \neq 0$ the preferred model of the universe is nearly a flat one, which is in agreement with CMBR data. It is an advantage of our GCG model as compared with Λ CDM model where in (1) high negative value of Ω_k was obtained as a best fit, although zero value of Ω_k was statistically admissible.

In order to find the curvature of the Universe they additionally used the data from CMBR and extragalactic astronomy. Another advantage of GCG model is that in natural way we obtained the conclusion that matter (barionic) component should be small what is in agreement with prediction from BBN (Big Bang Nucleosynthesis).

Density distribution functions (one dimensional PDF) for model parameters obtained by marginalization over remaining parameters of the model are presented in Figures 18-22. For Ω_k we obtain the limit $\Omega_k \in (-0.98, -0.22)$ at the confidence level 68.3% and $\Omega_k \in (-1, 0.23)$ at the confidence level 95.4%. For α and A_0 parameters we obtain the following results: $\alpha = 0$. and $A_0 = 0.89$ with the limit $\alpha \in (0, 0.64)$ and $A_0 \in (0.82, 1)$ at the confidence level 68.3% and $\alpha \in (0., 0.95)$ and $A_0 \in (0.73, 1.)$ at the confidence level 95.4%. For the density parameter Ω_{Ch} we obtain the limit $\Omega_{Ch} \in (0.87, 1.51)$ at the confidence level 68.3% and $\Omega_{Ch} \in (0.61, 1.79)$ at the confidence level 95.4%. For the density parameter Ω_m we obtain the limit $\Omega_m < 0.29$ at the confidence level 68.3% and $\Omega_m < 0.53$ at the confidence level 95.4%.

4. Generalized Chaplygin Gas model in perspective of SNAP data

In the near future the SNAP mission is expected to observe about 2000 SN Ia supernovae each year, over a period of three years¹. Therefore it could be possible to discriminate between various cosmological models since errors in the estimation of model parameters would decrease significantly.

We tested how a large number of new data would influence the errors in estimation of model parameters. We assumed that the Universe is flat and tested three classes of cosmological models. In the first Λ CDM model we assumed that $\Omega_m = 0.25$, and $\Omega_\Lambda = 0.75$ and $\mathcal{M} = -3.39$ (10). Second class was representative of the so called Cardassian models (23) with parameters $\Omega_m = 0.42$, $\Omega_{card} = 0.52$ and $n = -0.77$ as obtained in (24). The last model is Generalised Chaplygin Gas Model with parameters obtained in the present paper as best fits for the K3 sample ($\Omega_m = 0$, $A_0 = 0.85$, $\alpha = 1.$). Alternatively, we also test the Generalised Chaplygin Gas Model with parameters suggested by analysis of the Permmutter sample C ($\Omega_m = 0$, $A_0 = 0.76$, $\alpha = 0.40$).

For three above mentioned models we generated a sample of 1915 supernovae (Samples X1,X2,X3a,X3b respectively) in the redshift range $z \in [0.01, 1.7]$ distributed as predicted SNAP data (see TAB I of (25)) We assumed Gaussian distribution of uncertainties in the measurement of m and z . The errors in redshifts z are of order $1\sigma = 0.002$ while uncertainty

¹<http://www-supernova.lbl.gov>, <http://snfactory.lbl.gov>

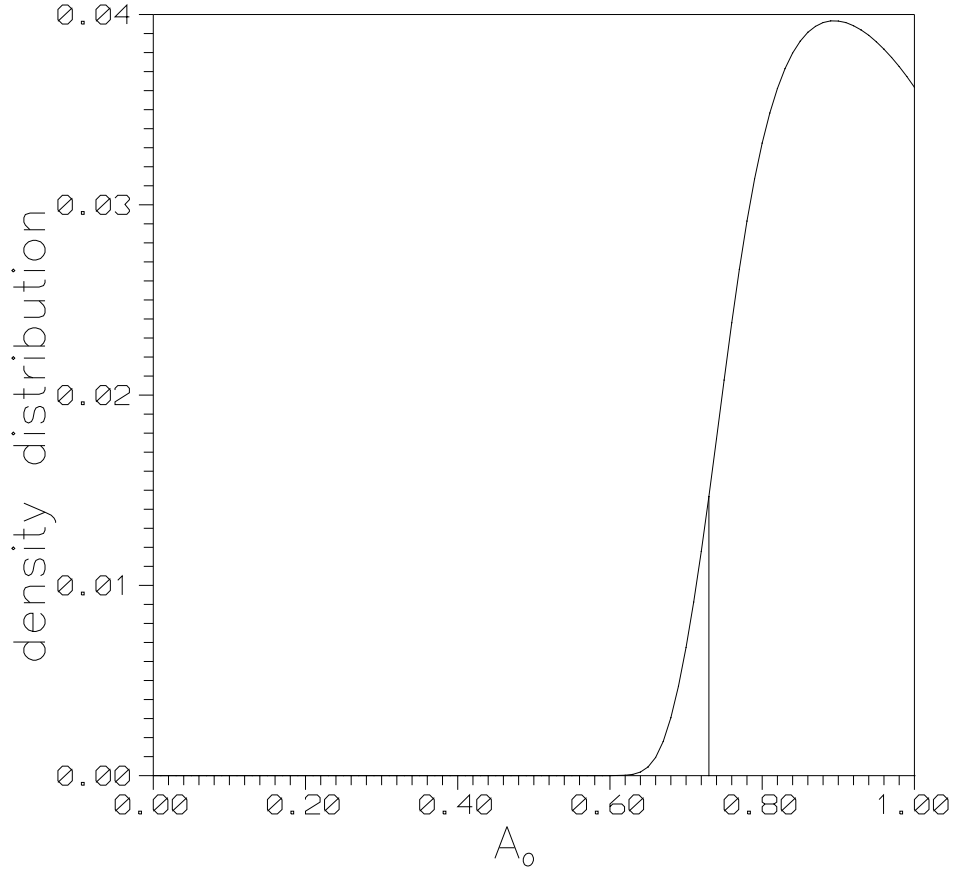


Fig. 19.— The density distribution (one dimensional PDF) for A_0 obtained from sample K3 by marginalization over remaining parameters of the model. We obtain the limit $A_0 \in (0.73, 1)$ at the confidence level 95.4%. (NON-flat GCG model.)

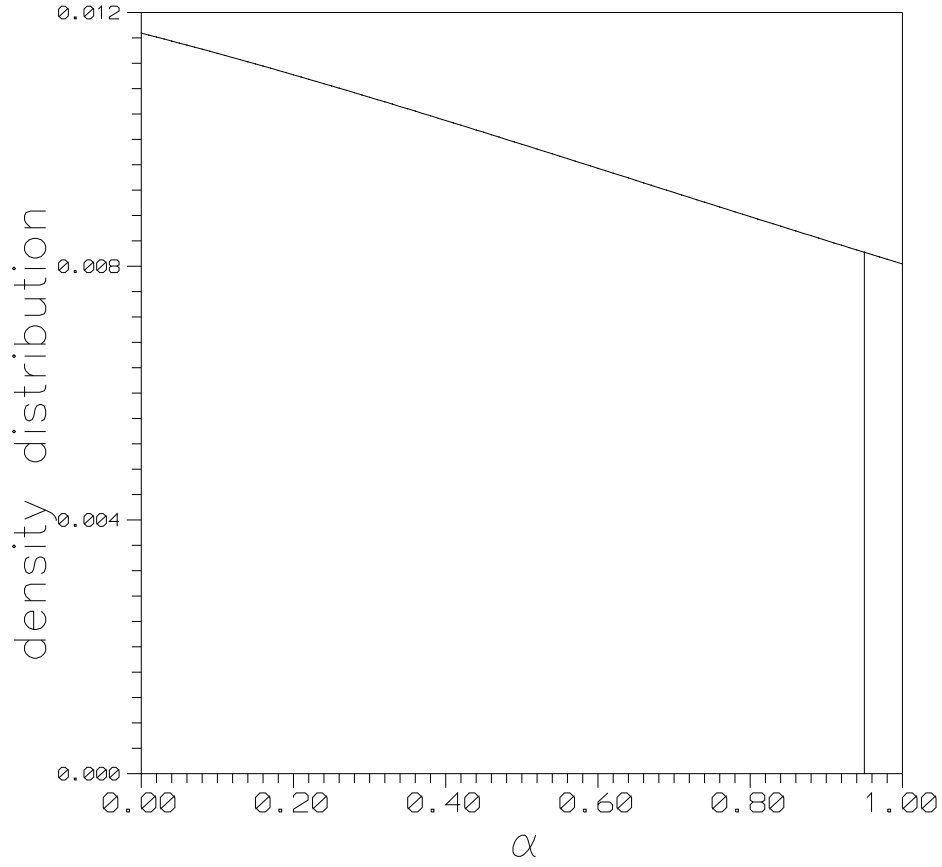


Fig. 20.— The density distribution (one dimensional PDF) for α obtained from sample K3 by marginalization over remaining parameters of the model. We obtain the limit $\alpha < 0.95$ at the confidence level 95.4%. (NON-flat GCG model.)

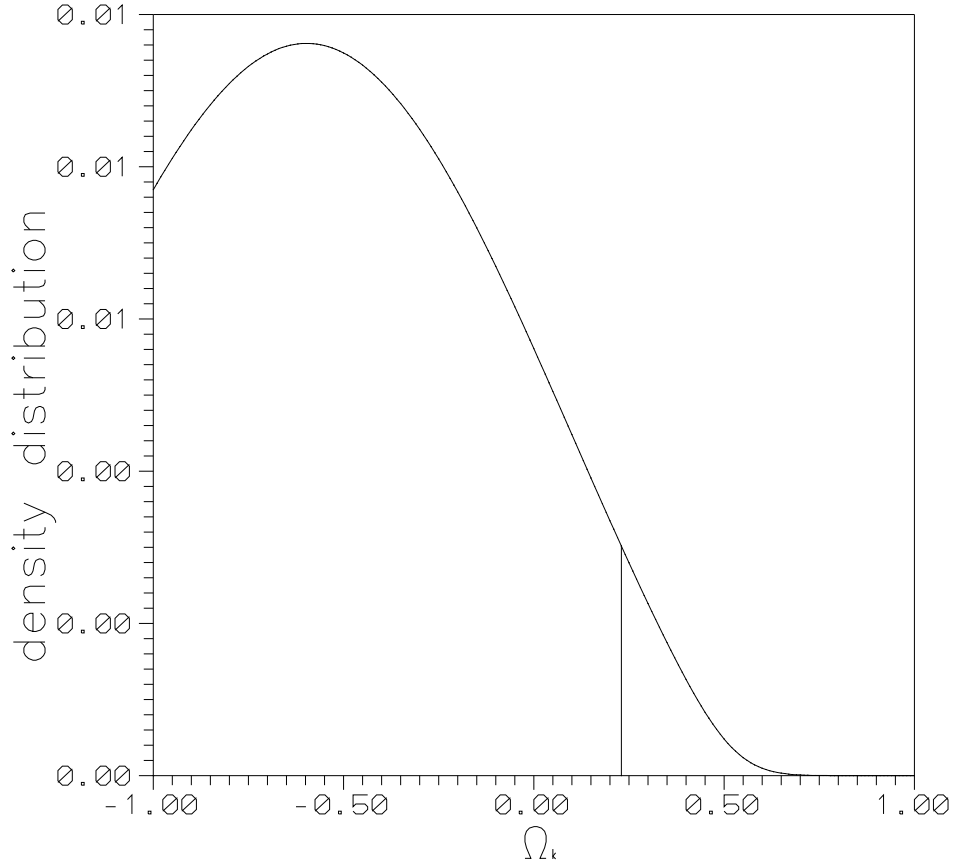


Fig. 21.— The density distribution (one dimensional PDF) for Ω_k obtained from sample K3 by marginalization over remaining parameters of the model. We obtain the limit $\Omega_k \in (-1, 0.23)$ at the confidence level 95.4%. (NON-flat GCG model.)

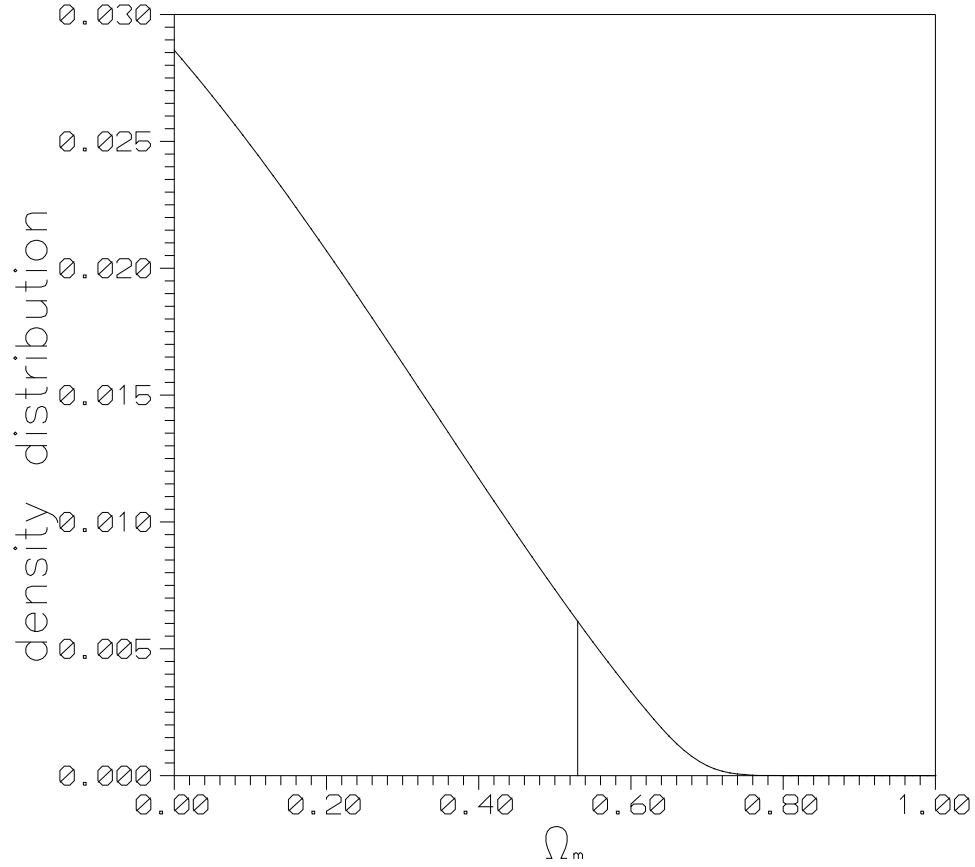


Fig. 22.— The density distribution (one dimensional PDF) for Ω_m obtained from sample K3 by marginalization over remaining parameters of the model. We obtain the limit $\Omega_m \in (0, 0.53)$ at the confidence level 95.4%. (NON-flat GCG model.)

in the measurement of magnitude m is assumed $1\sigma = 0.15$. The systematic uncertainty limits is $\sigma_{sys} = 0.02$ mag at $z = 1.5$ (25) that means that $\sigma_{sys}(z) = (0.02/1.5)z$.

For such generated sample we should now repeat our analysis. The result of our analysis is presented on figures Fig.23-26.

On that figures we present confidence levels on the plane (A_0, α) for sample of simulated SNAP data. The figures show the ellipses of preferred values of A_0 and α . It is easy to see that with the forthcoming SNAP data it will be possible to discriminate between predictions of Λ CDM and GCG models. With Cardasian Model the situation is not so clear, however (see Fig 24 and 25). Note that if $\alpha \simeq 0.4$ (as is suggested by analysis of Perlmutter sample C, see also (12)) then it will be possible to discriminate between model with Chaplygin gas and Cardasian model (see Fig 24 and 26). Moreover, it is clear that with the future SNAP data it would be possible to differentiate between models with various value of α parameter.

5. Conclusions

Generalized Chaplygin gas models have been intensively studied in the literature and in particular they have been tested against supernovae data (12), lensing statistics (13), CMBR measurements (14), age-redshift relation (15), x-ray luminosities of galaxy clusters (16) or from the large scale structure considerations (17). Although the results are in general mutually consistent there was no strong convergence to unique values of A_0, α parameters characterizing Chaplygin gas equation of state.

The authors of (12) have considered the FRW model filled completely with generalized Chaplygin gas and concluded that whole class of such models is consistent with current SNIa data although the value of $\alpha = 0.4$ is favoured. This result has been confirmed by our analysis (class (3) models). However, when the existing knowledge about baryonic matter content of the Universe was incorporated into the study our results were different from (12) who found that $\alpha = 0.15$ was preferred (assuming $\Omega_m = 0.04$ which is very close to our assumption for class (2) models).

As noticed by (17) generalized Chaplygin gas models have an inherent degeneracy with cosmological constant models as far as background evolution is concerned, and therefore they have a good fit with SNIa data. These degeneracies disappear at the level of evolution of perturbations and hence confrontation with CMBR spectrum would be decisive. Using available data on the position of CMBR peaks measured by BOOMERANG and Archeops (2; 3) Bento et al. (14) obtained the following constraints: $0.81 \leq A_0 \leq 0.85$ and $0.2 \leq \alpha \leq 0.6$ at 68% CL in the model representative of our class (2) (i.e. with $\Omega_m = 0.05$ assumed).

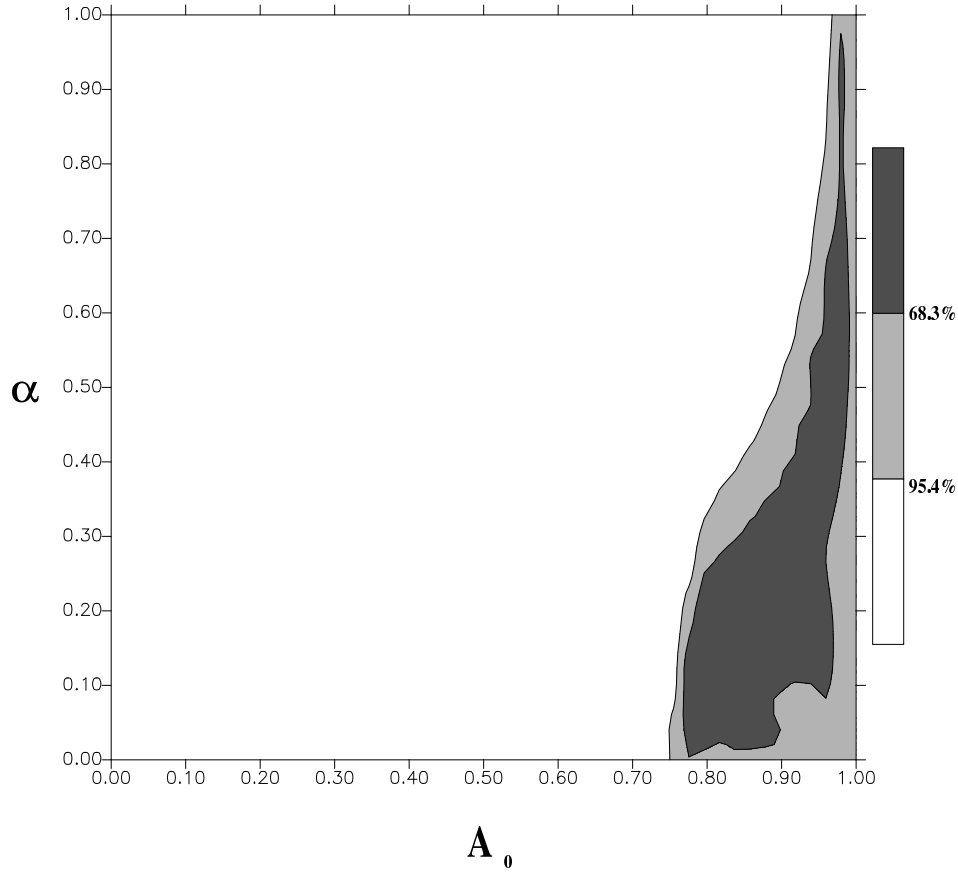


Fig. 23.— Confidence levels on the plane (A_0, α) for sample X1 (Λ CDM model) of simulated SNAP data, marginalized over Ω_m . The figure shows the ellipses of preferred values of A_0 and α .

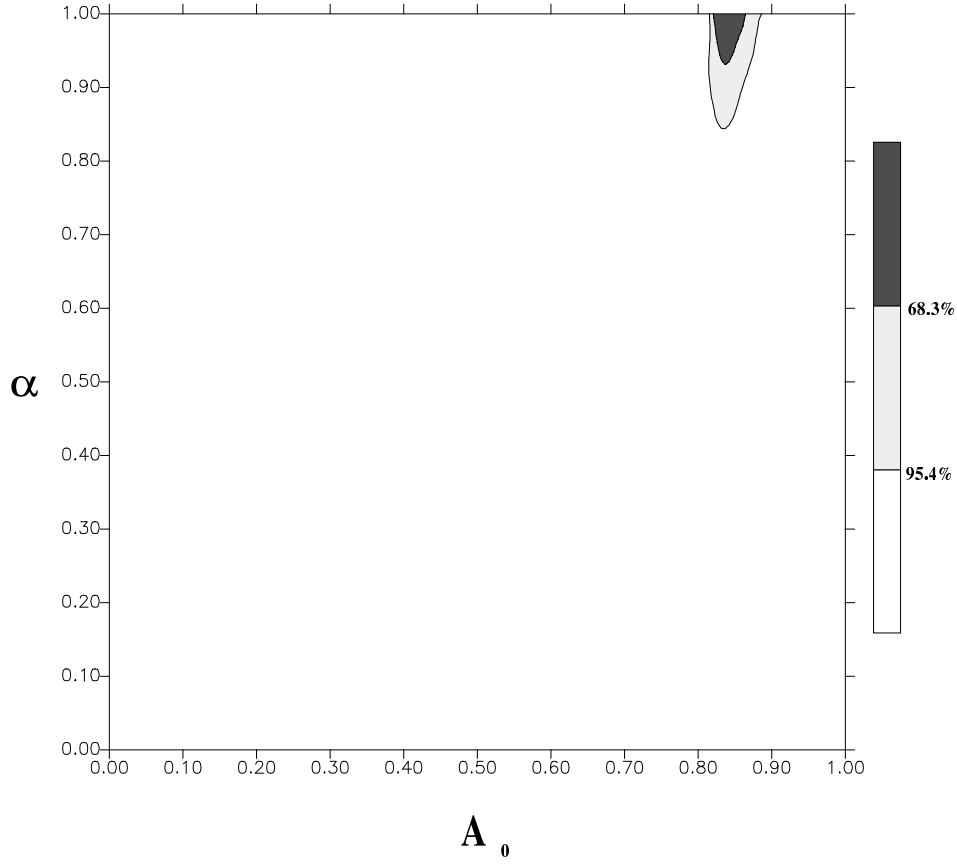


Fig. 24.— Confidence levels on the plane (A_0, α) for sample X2 (Cardassian model) of simulated SNAP data, marginalized over Ω_m . The figure shows the ellipses of preferred values of A_0 and α .

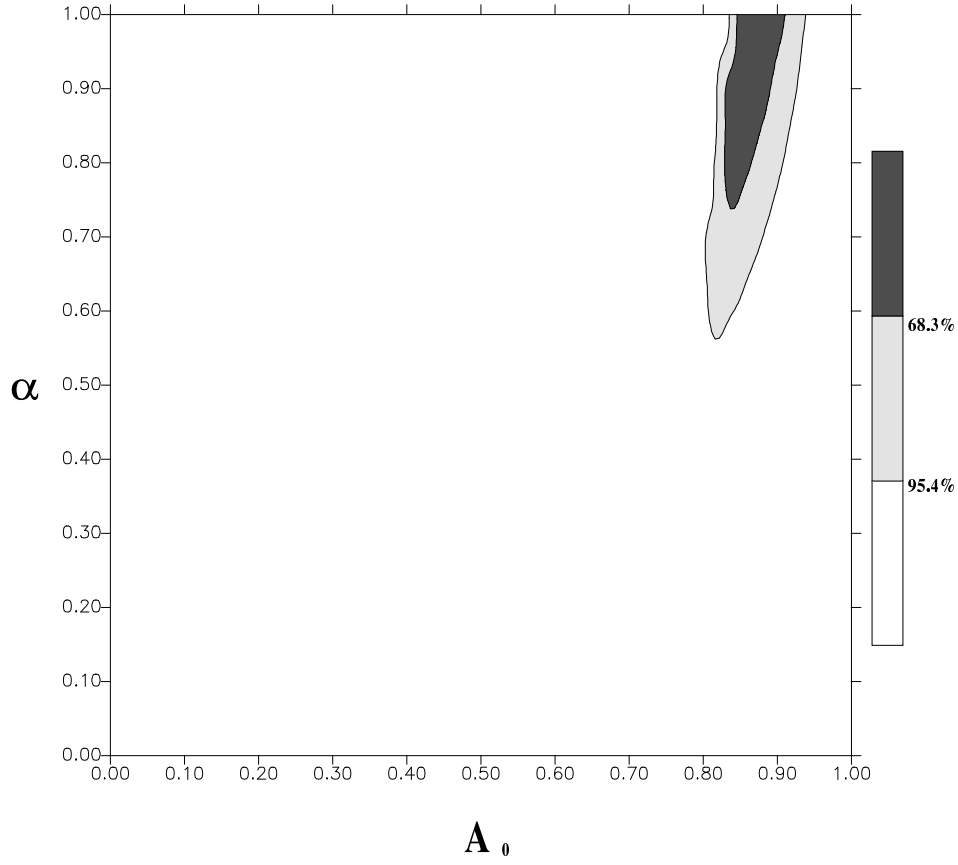


Fig. 25.— Confidence levels on the plane (A_0, α) for sample X3a (Generalized Chaplygin Gas model) of simulated SNAP data ($\Omega_m = 0$, $A_0 = 0.85$, $\alpha = 1.$), marginalized over Ω_m . The figure shows the ellipses of preferred values of A_0 and α .

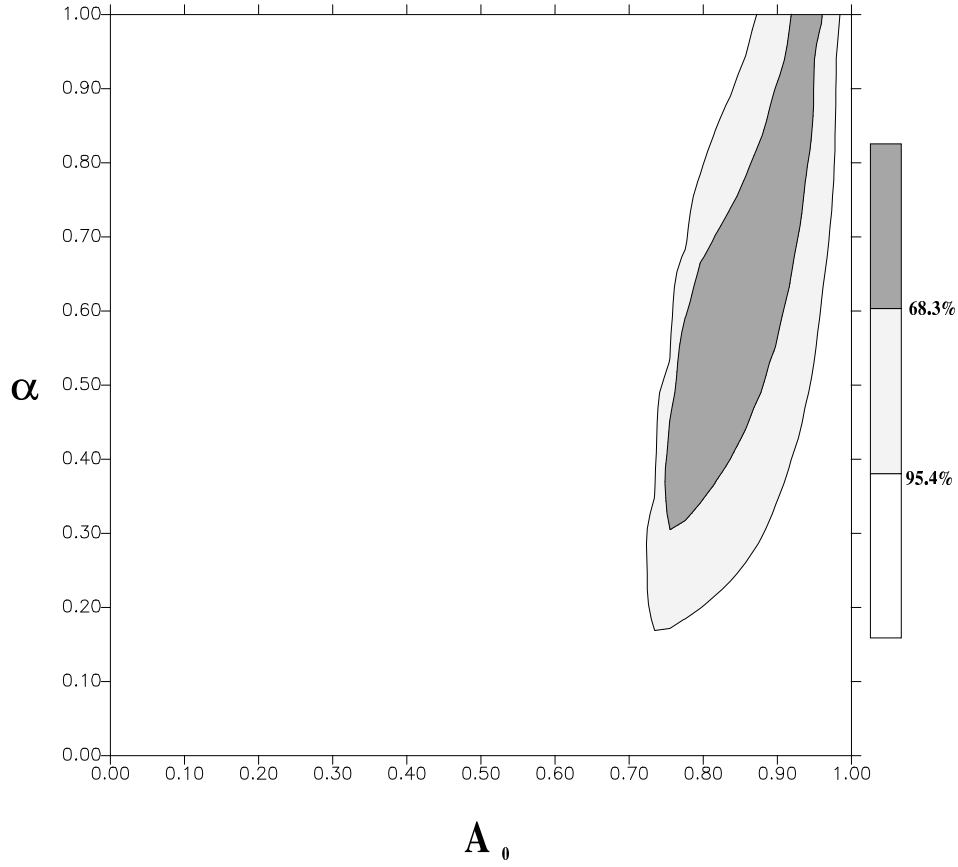


Fig. 26.— Confidence levels on the plane (A_0, α) for sample X3b (Generalized Chaplygin Gas model) of simulated SNAP data ($\Omega_m = 0$, $A_0 = 0.76$, $\alpha = 0.49$), marginalized over Ω_m . The figure shows the ellipses of preferred values of A_0 and α .

This result is consistent with ours derived from the sample C. Although the outliers often suggest statistical inhomogeneity of the data (and some hints suggesting the necessity of removing them from sample A exist) there is always a danger that removal of outliers is to some extent subjective. Therefore we retained the analysis of the full sample A in our analysis.

Using the angular size statistics for extragalactic sources combined with SNIa data it was found in (18) that in the the $\Omega_m = 0.3$ and $\Omega_{Ch} = 0.7$ scenario best fitted values of model parameters are $A_0 = 0.83$ and $\alpha = 1$. respectively.

Recent paper (19) in which Generalized Chaplygin gas models have been analyzed against Tonry et al. (20) supernovae data relaxing the prior assumption on flatness suggests, surprisingly as the authors admit, the preference of $\alpha > 1$.

In our analysis we have used Perlmutter data and a new Knop sample (10) because Knop discussed very carefully extinction correction. Consequently his sample has correctly assessed extinction. Therefore we believe that conclusions derived from Knop’s sample would be reliable. Analogous analysis on Tonry/Barris samples supported this result, although the accuracy was lower.

Our analysis suggests that SNIa data support the Chaplygin gas (i.e. $\alpha = 1$) scenario when the χ^2 fitting procedure is used. Quite unexpectedly, however, the maximum likelihood fitting prefers $\alpha = 0$ i.e. the cosmological constant scenario.

Extending our analysis by relaxing the flat prior lead to the result that even though the best fitted values of Ω_k are formally non-zero, still they are close to flat case. It should be viewed as an advantage of the GCG model since in similar analysis of Λ CDM model in (1) high negative value of Ω_k were found to be best fitted to the data and independent inspiration from CMBR and extragalactic astronomy has been invoked to fix the curvature problem. Another advantage of GCG model is that in natural way we obtained the conclusion that matter (barionic) component should be small what is in agreement with prediction from BBN (Big Bang Nucleosynthesis).

The results are dependent both on the sample chosen and on the prior knowledge of \mathcal{M} in which the Hubble constant and intrinsic luminosity of SNIa are entangled. Moreover the observed preference of A_0 values close to 1 means that the α dependence becomes insignificant (see equation (10)). It is reflected on one dimensional PDFs for α which turned out to be flat meaning that the power of the present supernovae data to discriminate between various Generalized Chaplygin gas models is weak. However, we argue that with the future SNAP data it would be possible to differentiate between models with various value of α parameter.

Residual plots indicate the differences between Λ CDM and Generalized Chaplygin Gas cosmologies at high redshifts. It is evident that Generalized Chaplygin Gas models have brighter supernovae at redshifts $z > 1$. Indeed one can see on respective figures (Fig.1, Fig.4, Fig.7, Fig.13) that systematic deviation from the baseline Einstein de Sitter model gets larger at higher redshifts. Therefore one can expect that future supernova experiments e.g. SNAP) having access to higher redshifts will eventually resolve the issue whether the dark energy content of the Universe could be described as a Chaplygin gas. The discriminative power of forthcoming SNAP data has been illustrated on respective figures (Fig.23-26) obtained from the analysis on simulated SNAP data.

6. Acknowledgements

We thank dr Barris for explanation of details of his SNIa sample. MS was supported by KBN grant no 2P03D00326

REFERENCES

- Perlmutter S., Aldering G., Goldhaber G., et al., *Astrophys.J* **517**, 565, 1999
Riess A., Filipenko A.V., Challis P., et al., *Astron.J* **116**, 1009, 1998
- deBernardis P. et al., *Nature* **404**, 955, 2000
- Benoit A., et al., *Astron.Astrophys.* **399**, L25-L30, 2003
Hinshaw G. et al. [WMAP collaboration], 2003, ApJ submitted; astro-ph/0302217
- Turner M., *Astrophys.J* **576**, L101-L104, 2002
- Ratra B., Peebles P.J.E., *Phys.Rev.D* **37**, 3406, 1988
Caldwell R.R., Dave R., Steinhardt P.J., *Phys. Rev. Lett.* **75**, 2077, 1995
Frieman J., Hill C., Stebbins A., Waga I., *Phys. Rev. Lett.* **75**, 2077, 1995
- Kolda C., Lyth D., *Phys.Lett. B* **458**, 197, 1999
- Kamenshchik A., Moschella V., Pasquier V., *Phys.Lett. B* **511**, 256, 2000;
Fabris J.C., Gonçalves S.V.B., de Souza P.E., *Gen.Relat.Grav.* **34**, 53, 2002
Szydlowski M., Czaja W. *Phys.Rev. D* **69**, 023506, 2004
- Ogawa N., *Phys.Rev. D* **62**, 085023, 2000

- Bento M.C., Bertolami O., Sen A.A., *Phys.Rev. D* **66**, 043507, 2002
Carturan D., Finelli F., 2002 astro-ph/0211626v1
- Knop R. A. et al. , *Astrophys.J* **598**, 102, 2003; astro-ph/0309368
- Peebles P. J. E., Ratra B., *Rev. Mod. Phys.***75**, 559 2003
- Makler M., de Oliveira S.Q., Waga I., *Phys.Lett. B* **555**, 1, 2003
Avelino P.P., Beça L.M.G., de Carvalho J.P.M., Martins C.J.A.P., Pinto P., *Phys. Rev. D* **67**, 023511, 2003
Fabris J.C., Gonçalves S.V.B., de Souza P.E., astro-ph/0207430
Collistete Jr. R., Fabris J.C., Gonçalves S.V.B.,de Souza P.E., astro-ph/0303338
- Dev A., Alcaniz J.S., Jain D., *Phys. Rev. D* **67**, 023515, 2003
Silva P.T., Bertolami O., astro-ph/0303353
- Bento M.C., Bertolami O., Sen A.A., *Phys.Rev. D* **67**, 063003, 2003
Bento M.C., Bertolami O., Sen A.A., *Phys.Lett. B* **575**, 172–180, 2003
Carturan D., Finelli F., *Phys.Rev. D* **68**, 103501, 2003
Amendola L., Finelli F., Burigana C., Carturan D., *JCAP* **0307**, 5, 2003
- Alcaniz J.S., Jain D., Dev A., *Phys. Rev. D* **67**, 043514, 2003
- Cunha J.V., Lima J.A.S., Alcaniz J.S., astro-ph/0306319
- Bean R., Doré O., *Phys. Rev. D* **68**, 023515, 2003
Multamaki T., Manera M., Gaztanaga E., astro-ph/0307533
Bilic N., Lindenbaum R.J., Tupper G.B., Viollier R.D., astro-ph/0307214
- Alcaniz J.S., and Lima J.A.S., astro-ph/0308465, 2003
- Bertolami O., Sen A.A., Sen S., Silva P.T., astro-ph/0402387
- Tonry J.L., et al., *Astrophys.J* **594**, 1, 2003
- Barris B. J. et al. 2003 astro-ph/0310843
- Williams B. F. et al. 2003 astro-ph/0310432
- Freese K., Lewis M., *Phys. Lett. B* **540**, p1 2002
- Godłowski W., Szydlowski M., Krawiec A., *Astrophys.J* **605**, 599, 2004, astro-ph/0309569
- Alam U. et al., 2003, astro-ph/0303009

